# SAND AND DUST STORM WARNING ADVISORY AND ASSESSMENT SYSTEM (SDS-WAS)

## EVALUATION OF DUST PREDICTION MODELS

**Enric Terradellas (AEMET), José M. Baldasano (BSC-CNS), Emilio Cuevas (AEMET), Christos Spyrou, Jonilda Kushta and George Kallos (NKUA)**

**19 February 2014**
**Draft**

**WMO Research Department**

**Atmospheric Research and Environment Branch**

**Index**

## 1. Background

The evaluation of a mineral dust model output is an essential step before establishing an operational dust forecasting and early warning system based on numerical simulations. The evaluation is aimed at providing information on the model capabilities, limitations, and appropriateness for the purpose for which it was designed. Its main goal is to evaluate the accuracy in the simulation of the dust content in the atmosphere. Secondary goals include assessment of the suitability of a specific application and configuration and guidance for improvement. The model evaluation is based on the comparison of the model results with observational data.

## 2. Observational data

The major problem in the evaluation of dust models is the scarcity of relevant observations, especially near the main dust sources, in desert and unpopulated areas. The main data sources come from:

- Air-quality monitoring stations
- Visibility observations from meteorological reports
- Sun-photometers
- Lidar
- Satellite remote sensing

### 2.1 Air quality monitoring stations

Since the air quality monitoring networks perform in-situ measurements, they could be the main data source for point evaluation of dust surface concentration. It is necessary to bear in mind that these measurements integrate the contribution of the different types of atmospheric aerosol and that routine observations are usually limited to the concentration of particulate matter with an aerodynamic diameter less than 10 micrometers (PM10)(see an example of a monthly PM10 record in Figure 1). The main problems of this kind of measurements are:

- Lack of stations near the dust source regions
- Networks are usually designed to monitor air pollution in urban or industrial areas, which are dominated by anthropogenic particles.
- Lack of international regulations for data exchange

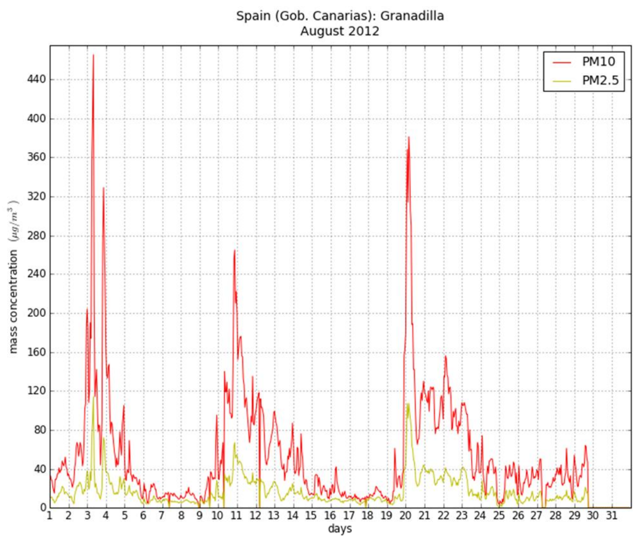

Fig. 1: PM10 and PM2.5 records from Granadilla (Canary Islands, Spain) for August 2012 clearly show three Saharan dust outbreak.

### 2.2 Visibility observations from meteorological reports

Visibility data included in meteorological reports (Figure 2) have sometimes been used as an alternative way to evaluate dust forecasts (Shao et al., 2003). Visibility data must be complemented with information on present weather to discard those cases where visibility is reduced by the presence of hydrometeors. There are several empirical relationships between visibility and dust surface concentration in the literature (dôAlmeida, 1986; Ben Mohamed et al., 1992; Shao et al., 2003). However, their validity is very limited, because the visibility reduction not only depends on the dust concentration, but also on the size, density, chemical and mineralogical composition of particles as well as on atmospheric humidity.

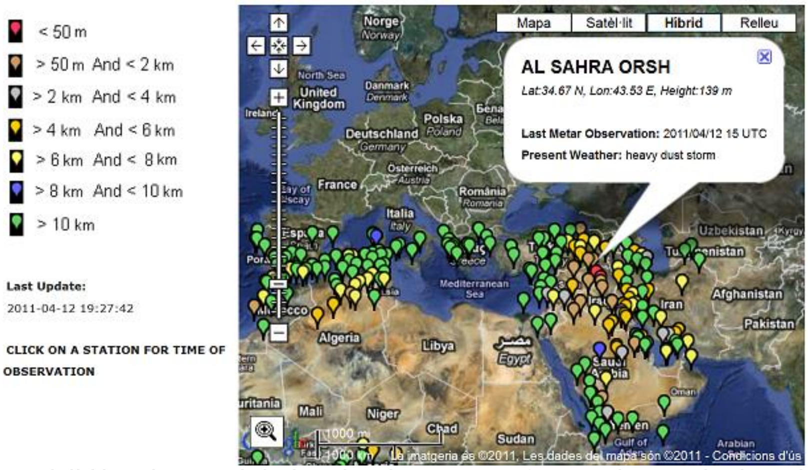


Fig. 2: Low visibility observed during the dust event of 12 April 2011 in the Middle East

### 2.3 Sun-photometers

Direct sun-photometric measurements are a powerful remote sensing tool that provides retrieval of column-integrated aerosol microphysical and optical properties, which are very useful for point model evaluation. The Aerosol Robotic Network (AERONET) is a comprehensive network that provides near-real-time datasets of aerosol properties (Holben et al., 1998; Dubovik and King, 2000). The aerosol optical depth (AOD) integrates the contribution of different aerosol types, but can be complemented with spectral information that yields information on the aerosol composition (Figure 3). A major shortcoming of these measurements is their unavailability under cloudy skies and during nighttime and lack of information on the vertical aerosol distribution. However, these measurements are by far the most commonly used in dust model evaluation.

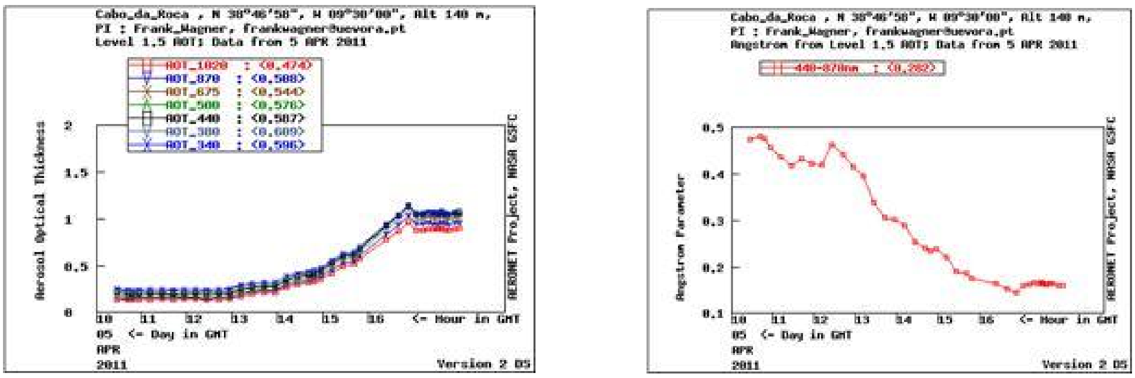

Fig. 3: Progressive increase of AOD and decrease of the 440-870 nm-Angström exponent (AE) indicating a dust outbreak in Cabo da Roca, Portugal, on 5 April 2011.

### 2.4 Lidar

Lidar and the latest generation of ceilometers permit routine measurement of aerosol vertical profiles. However, continuous measurements in ground-based stations are only performed in a few stations that are, in general, far from the main dust sources.

### 2.5 Satellite remote-sensing

The satellite products have the advantage of a large spatial coverage and a regular and quick availability. However, satellite measurements are highly integrated both over the atmospheric column and over all aerosol components and, in the visible part of the electromagnetic spectrum, show a limited detectability over bright surfaces such as deserts, which are the main dust sources. A new generation of infrared spectrometers and interferometers such as those set onboard the AIRS and IASI satellites have great potential for dust observation (Hilton et al., 2012), but the algorithms are still under development (Peyridieu, et al 2010, Klüser et al, 2011). Ultra-violet measurements as used in the MODIS Deep Blue algorithm allows a retrieval of aerosol optical depth over bright surfaces, which can be translated into a visible aerosol optical depth (Hsu et al., 2006; Ginoux et al., 2010, 2012).

## 3. Evaluation of dust models at the Regional Center for Northern Africa, Middle East and Europe of the WMO SDS-WAS program

The exchange of forecast products is recognized as a core part of the Implementation Plan of the WMO SDS-WAS programme and as a basis for the joint evaluation initiative. It is done for the ñReference Areaò (RA), from 25°W to 60°E in longitude and from 0° to 65°N in latitude, which is intended to cover the main source areas in Northern Africa and Middle East, as well as the main transport routes and deposition zones from the equator to the Scandinavian Peninsula. The action involves three-hourly forecasts of up to 72h with a 3-hour frequency, involving the following variables:

- Dust concentration at surface
- Dust optical depth (DOD) at 550 nm

At the end of 2012, seven models participated in the initiative by sending daily files with numerical outputs:

| Model | Institution |
|---|---|
| BSC-DREAM8b_v2 | Barcelona Supercomputing Center ï National Supercomputing Center (BSC-CNS) |
| MACC-II | European Center for Medium-Range Weather Forecast (ECMWF) |
| DREAM8-NMME-MACC | South Eastern European Virtual Climate Change Center (SEEVCCC) |
| NMMB/BSC-Dust | Barcelona Supercomputing Center ï National Supercomputing Center (BSC-CNS) |
| MetUM | U. K. Met Office |
| GEOS-5 | U. S. National Aeronautics and Space Administration (NASA) |
| NGAC | National Centers for Environmental Prediction (NCEP) |

Two other models have also been involved during specific periods:

| Model | Institution |
|---|---|

| | |
|---|---|
| LMDzt-INCA | French Climate and Environment Sciences Laboratory (LSCE) |
| CHIMERE | French Laboratory of Dynamical Meteorology (LMD) |

The values of dust surface concentration and DOD provided by each model are daily plotted side-by-side for the reference area using a common color palette. The palette has been built by combining brownish and greenish colours. The brownish tones highlight the areas with the highest contents of mineral dust whereas the greenish tones allow emphasizing the thresholds set by European Union directives on air quality. The latest forecast, as well as historical plots, is available at:

http://sds-was.aemet.es/forecast-products/compared-dust-forecasts

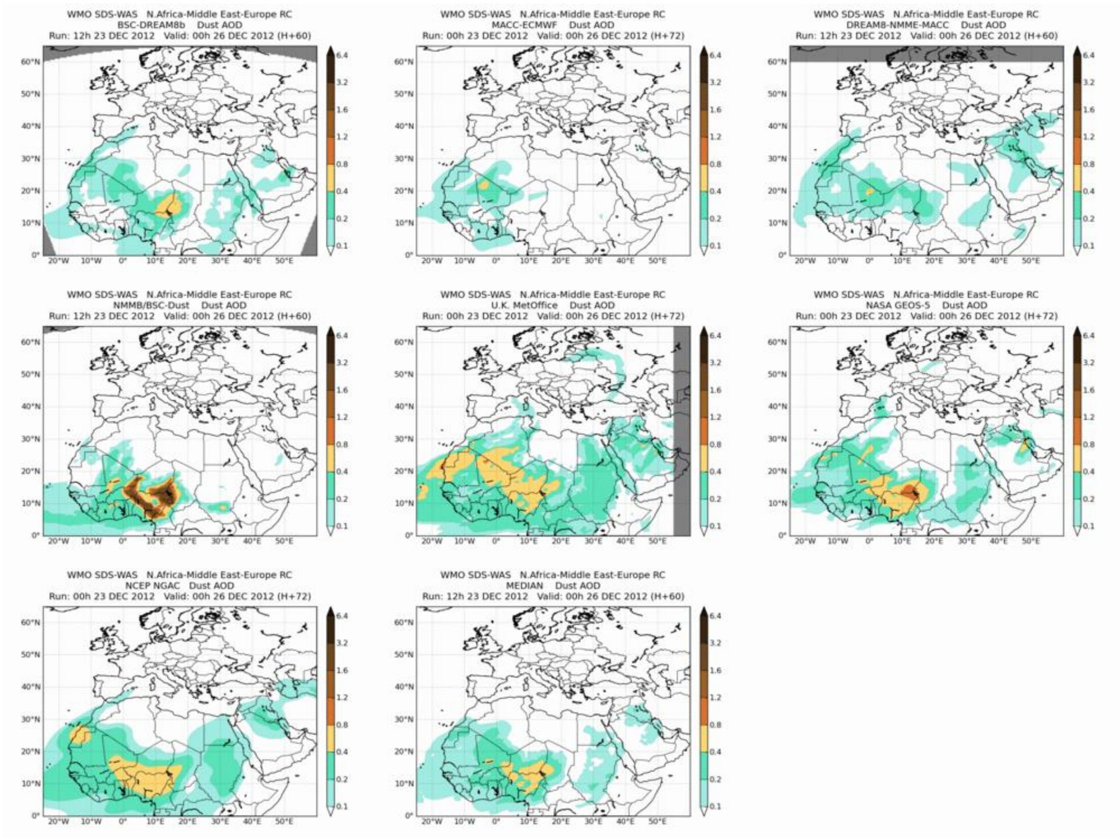


Fig. 4: Dust AOD forecast by different models for 00 UTC 26 December 2012

The Regional Centre daily generates multi-model products for the Reference Area using the results of the above mentioned models: http://sds-was.aemet.es/forecast-products/dust-forecasts/multimodel-products. In particular, the multi-model median forecasts of dust surface concentration and DOD are plotted along with their corresponding single-model elements.

The DOD at 550 nm forecast by the models and multi-model median is then drawn together with the AERONET observations of AOD in monthly charts for the 40 selected dust-prone stations indicated in Figure 5. Monthly plots are daily updated and automatically archived: http://sds-was.aemet.es/forecast-products/forecast-evaluation. These plots, implemented for near-real-time (NRT) monitoring, are very valuable to detect outliers and to identify jumps in performance. Figure 6 clearly shows how the different models are able to simulate the dust outbreaks over Tenerife (Canary Islands) during August 2012.

The AERONET retrievals of AOD integrate the different sources of atmospheric aerosol. To minimize the sources of error, the comparison is restricted to situations in which mineral dust is the dominant aerosol type. Threshold discrimination is made by flagging observations with an Ångström exponent 440-870 higher than 0.6, which indicates the presence of smaller particles.


Fig. 5: AERONET stations used in the forecast evaluation

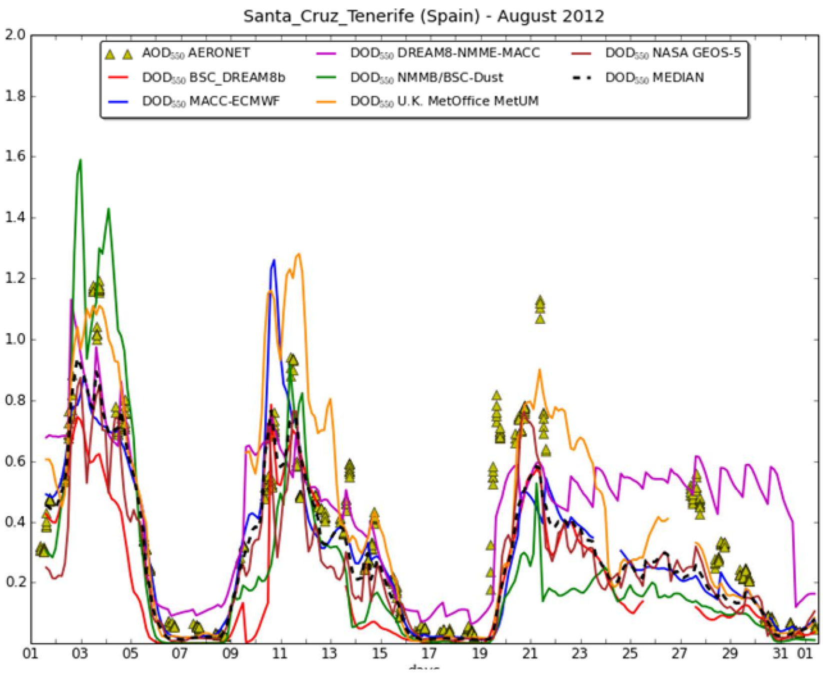


Fig. 6: DOD forecast by different models (full lines) and multi-model median (dashed black line) compared with AOD (yellow triangles) from the AERONET station of Santa Cruz de Tenerife (Canary Islands, Spain) in August 2012.

In addition to this NRT evaluation, a system to quantitatively assess the performance of the different models has been set up. The system yields evaluation scores computed from the comparison of the simulated DOD and the AERONET retrievals of AOD.

The common metrics used to quantify the departure between modeled ($c_i$) and observed ($o_i$) quantities are:

- The mean bias error (BE), which captures the average deviations between two datasets.
- The root mean square error (RMSE), which combines both the bias and the standard deviation. It is strongly dominated by the largest differences between observations and

model, due to the squaring operation. Especially in cases where prominent outliers occur, the usefulness of RMSE is questionable and the interpretation becomes difficult.

- The correlation coefficient (r), which indicates the extent to which patterns in the model match those in the observations.
- The fractional gross error (FGE), which is a measure of the overall model error. It ranges between 0 and 2 and behaves symmetrically with respect to under- and overestimation, without over emphasizing outliers.

| Statistic Parameter | Formula |
|---|---|
| Mean Bias Error (BE) | $BE = \frac{1}{n}\sum_{i=1}^{n}(c_i - o_i)$ |
| Root Mean Square Error (RMSE) | $RMSE = \sqrt{\frac{1}{n}\sum_{i=1}^{n}(c_i - o_i)^2}$ |
| Correlation coefficient (r) | $r = \frac{\sum_{i=1}^{n}(c_i - \bar{c})\cdot(o_i - \bar{o})}{\sqrt{\sum_{i=1}^{n}(c_i - \bar{c})^2}\cdot\sqrt{\sum_{i=1}^{N}(o_i - \bar{o})^2}}$ |
| Fractional Gross Error (FGE) | $FGE = \frac{2}{n}\sum_{i=1}^{n}\left\lvert\frac{c_i - o_i}{c_i + o_i}\right\rvert$ |

The scores of each model and multi-model median are computed on a monthly, seasonal and annual basis for each AERONET site, for three selected regions (Sahel/Sahara, Middle East and Mediterranean), as well as globally, considering all sites. It should be noted that scores for individual sites can have little significance for being calculated from a small number of data. It is also necessary to bear in mind that observed AOD always includes other particles than dust, so a small negative bias can be expected.

Monthly evaluation scores are available at http://sds-was.aemet.es/forecast-products/forecast-evaluation/model-evaluation-metrics, seasonal scores at http://sds-was.aemet.es/forecast-products/forecast-evaluation/model-evaluation-metrics-seasonal and, finally, annual scores at http://sds-was.aemet.es/forecast-products/forecast-evaluation/model-evaluation-metrics-annual.

## 4. Dust model operations and evaluations at NKUA/AM&WFG

The Atmospheric Modeling & Weather Forecasting Group of the National and Kapodistrian University of Athens (NKUA/AM&WFG) runs dust prediction model configurations since 1997. Two main modeling systems have been developed and run for both research and forecasting. These are the SKIRON/Dust and RAMS/ICLAMS. In both systems, the dust cycle sub-models are directly coupled with the meteorological driver while links and feedbacks between aerosol-radiation-cloud-precipitation interactions are incorporated. More information can be found below. The areas covered are North Africa, Mediterranean, Europe, Middle East, Arabian Peninsula, West and Central Asia with different resolutions, according to specific applications. The forecasting horizon is usually five days. Very high-resolution operational applications go down to 500x500 meters in two-way nesting configuration. Below we will provide model evaluation information of both models. Typical forecasts available in public domain can be found in http://forecast.uoa.gr. In this web page, relevant publications from the AM&WFG are available too.

## 4.1 SKIRON/Dust model Evaluation

The SKIRON/Dust modeling system is based on the atmospheric model SKIRON, which has been developed at the University of Athens from the Atmospheric Modelling and Weather Forecasting Group (Kallos et al., 1997; Nickovic et al., 2001; Kallos et al., 2006; Spyrou et al., 2010) in the framework of a number of projects (SKIRON, MEDUSE, ADIOS, CIRCE and recently MARINA Platform). A dust module that simulates the production and removal of the desert dust aerosol is directly coupled with the host model. The SKIRON atmospheric model includes several sophisticated parameterization schemes, such as the OSU (Oregon State University) scheme (Ek and Mahrt, 1991) for simulation of the surface processes, including a data assimilation scheme for soil temperature and soil wetness, and the option of choosing among Betts-Miller-Janjic (Betts, 1986) and Kain-Fritsch (Kain and Fritsch, 1990) convective parameterization schemes for the representation of moisture processes. During the SKIRON/Dust runs, the prognostic atmospheric and hydrological conditions are used in order to calculate the effective rates of the injected dust concentration based on the viscous/turbulent mixing, soil composition, soil moisture, shear-free convection and diffusion (Papadopoulos et al., 2002). The dust module includes a particle size distribution in order to simulate more accurately the size-dependent processes. In the current form of the modelling system, the transport mode uses eight size bins (log-normally distributed) with effective radius 0.15, 0.25, 0.45, 0.78, 1.3, 2.2, 3.8, 7.1 εm.

Recently, the modelling system was significantly upgraded in order to improve the model prediction efficiency meeting the current needs for accurate simulation of the mineral dust cycle and the interaction mechanisms with various atmospheric processes. New features include improvements in the description of the bottom boundary (ground or sea surface) characteristics of the atmospheric model and the dust aerosol properties (Spyrou et al., 2010). The new model version includes a 16-category soil characteristics dataset (Miller and White, 1998) that provides detailed information on soil physical properties, such as porosity and available water capacity. A high-resolution (30-second) global land use/land cover database including urban areas and classified according to the 24-category USGS land use/land cover system (Anderson et al., 1976) is utilized. For the more accurate description of the topographic variability that determines the incoming solar radiation reaching the surface, in the upgraded SKIRON/Dust model a new preprocessor was developed that derives statistics for the slope steepness and orientation, from the high resolution topography datasets. The dust aerosol is described by using the three-modal lognormal function of D'Almeida (1987) for the aerosol mass distribution at the source areas and the 8-size bin transport mode of Schulz et al. (1998) for the long-range transported particles. The dust particles are assumed to be mobilized through the process of saltation bombardment (Marticorena and Bergametti 1995) and deposited via dry (diffusion, impaction, gravitational settling) and wet (in-cloud and below-cloud removal) mechanisms. Lately the model has been updated to work with the RRTM radiative transfer code, in order to evaluate the direct radiative feedbacks of desert dust (Spyrou et al., 2013). More details on the specific characteristics of the atmospheric model are provided in Spyrou et al. (2010) and Mesinger et al. (2012).

## 4.2 Sensitivity test of the 17th of April 2005

A strong dust transort episode was examined during April 2005. On the 15th of April strong surface winds introduced large quantities of dust particles on the atmosphere. These particles were transported towards the Central and Eastern Europe. To evaluate the model scatterplots were created for three AERONET stations on the Mediterranean, in Crete, Lampedusa and Lecce (Figure 8).

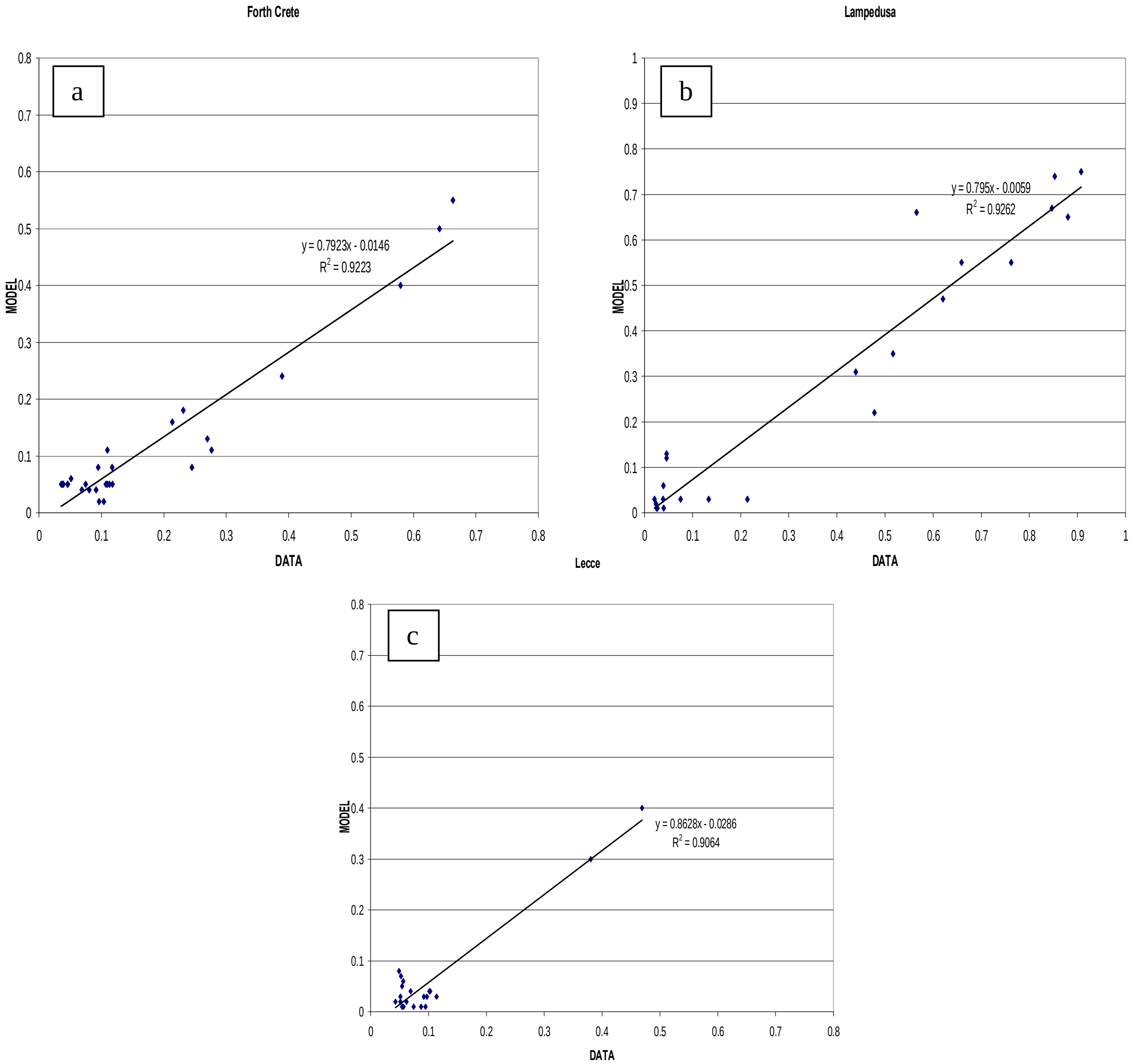


Figure 8: Observed and modeled scatterplots of the interpolated AOD at 550 nm for April 2005 at a) Crete, b) Lampedusa and c) Lecce.

The optical depth values observed vary from 0.1 on the 15th and 16th of April to 0.9 to the 17th and 18th, where the dust plume is fully extended over the Mediterranean (Figure 9). The largest values are observed over Lampedusa, which is the closest station on North Africa.

High correlation values were observerved for all the three stations along the path of the dust cloud. In Crete and Lampedusa station the correlation reached 0.95 and in Lecce 0.94. The underestimation of the model in all the cases is due to the fact that the model only calculates the natural particles effect and not the anthropogenic sources (Spyrou 2011).

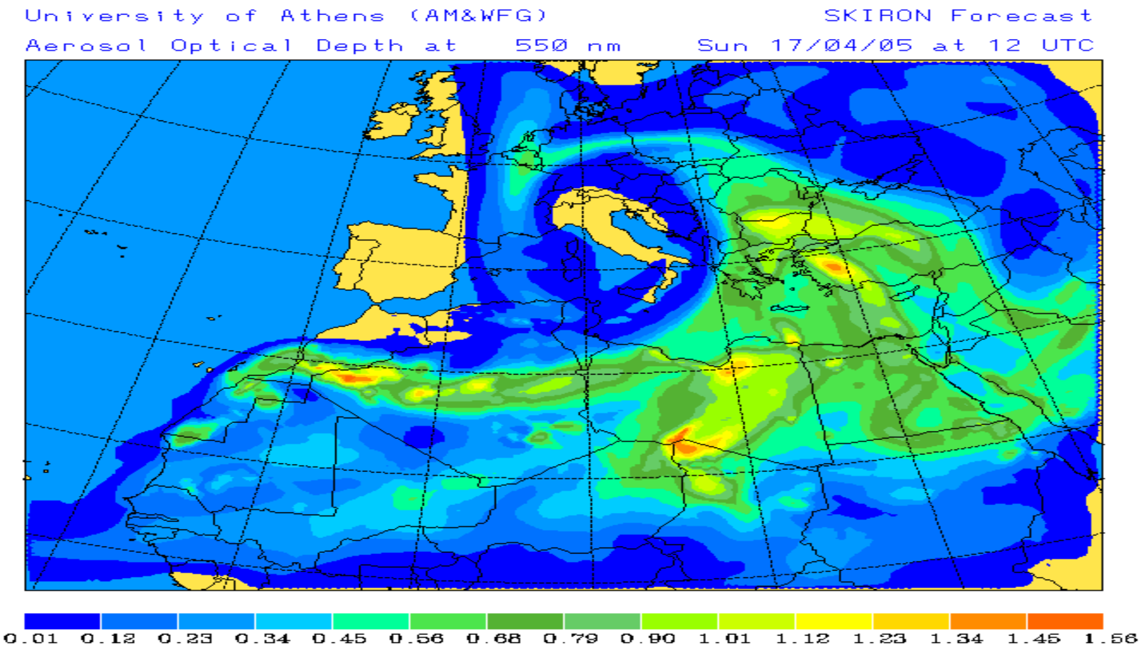


Figure 9: Modeled values of Aerosol Optical Depth at 550nm on the 17th of April 2005.

### 4.3 Dust concentration

Model estimates of near ground dust concentrations have been compared with $PM_{10}$ observations from three monitoring stations of the Israeli Ministry of the Environment (Beersheba: 31º 15′N, 34º 47′E, Afula: 32º 32′N, 35º 23′E, Modiin: 31º 54′N, 35º 00′E) and for the period covering April 2005. The time-series of mass concentration, as well as the scatter plots between predicted dust concentrations and measured $PM_{10}$ concentrations, are illustrated in Figure 10. The time-series plots exhibit considerable temporal coincidence of the maxima and minima for the compared datasets during the whole month period and in all three selected areas. Specifically, on the 22nd of April the particle mass concentration reached up to 280 εg m$^{-3}$ in Modiin, while the SKIRON model captured satisfactorily the observed values especially in Afula station. This agreement could possibly denote a dust event in the greater region. A stronger dust episode in the period between 8th and 10th of the month can be detected in the time-series of all monitoring sites. The model predicted the particle mass increase one day earlier, but the simulated intensity of the episode, expressed in terms of mass concentration, was very close to the observed one (Spyrou et al., 2010).

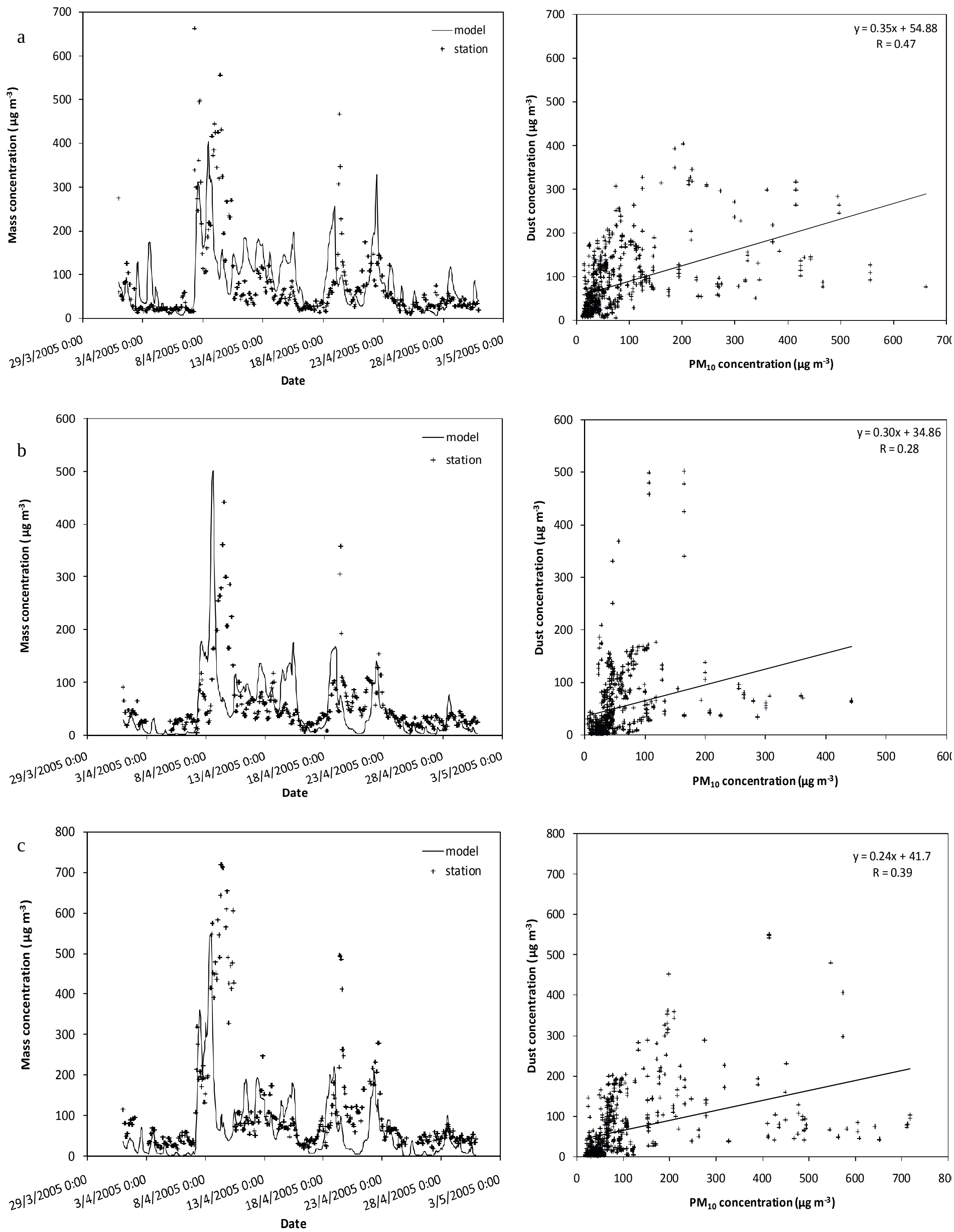


Figure 10: Time-series of the mass concentration and scatter plots between modeled dust and observed $PM_{10}$ concentration values for April 2005 at Israel monitoring stations: a) Beersheba, b) Afula and c) Modiin.

## 4.4 Aerosol Optical Depth

Model run AOD calculations at 532 nm were compared with measured values originating from sun photometer data of the AERONET network (level 1.5) over the periods of April of 2006 and May of 2008. During each spring period, at least two dust events occurred in a number of selected monitoring stations (Lampedusa, Crete, Athens, Blida and Tamanrasset), whose selection was based on the occurrence of dust load maxima during the studied periods and the representativeness of the dust affected Mediterranean areas. The level 2.0 quality controlled data of the network were not used in the present analysis since they were not available for all selected sites and periods (e.g. Crete for May 2008) and they included large gaps during dust episodes. The AOD values that correspond to 440 and 870 nm, provided by the AERONET network, were used for the calculation of the AOD at 532 nm for each monitoring station, following Perez et al., 2006. Figures 11 and 12 show the time-series of the AOD at 532 nm for the various monitoring sites and during the two aforementioned periods, as a function of the Julian day. The measured AOD reaches the value 0.8 over Greece (i.e. Crete, Athens) and in Lampedusa and exceeds the value 1 at the dust source area of Blida. In general, the model outputs follow the trend of the observational values in all selected areas and for some specific dust events, the simulated values are very close to the monitored ones. For example, the model captured quite well the dust episode that occurred in Greece in the end of May 2008. In other cases, the model captured correctly the onset of a dust episode, such as the one occurred in early April 2006 in Tamanrasset, but during the episode the AOD values were overestimated.

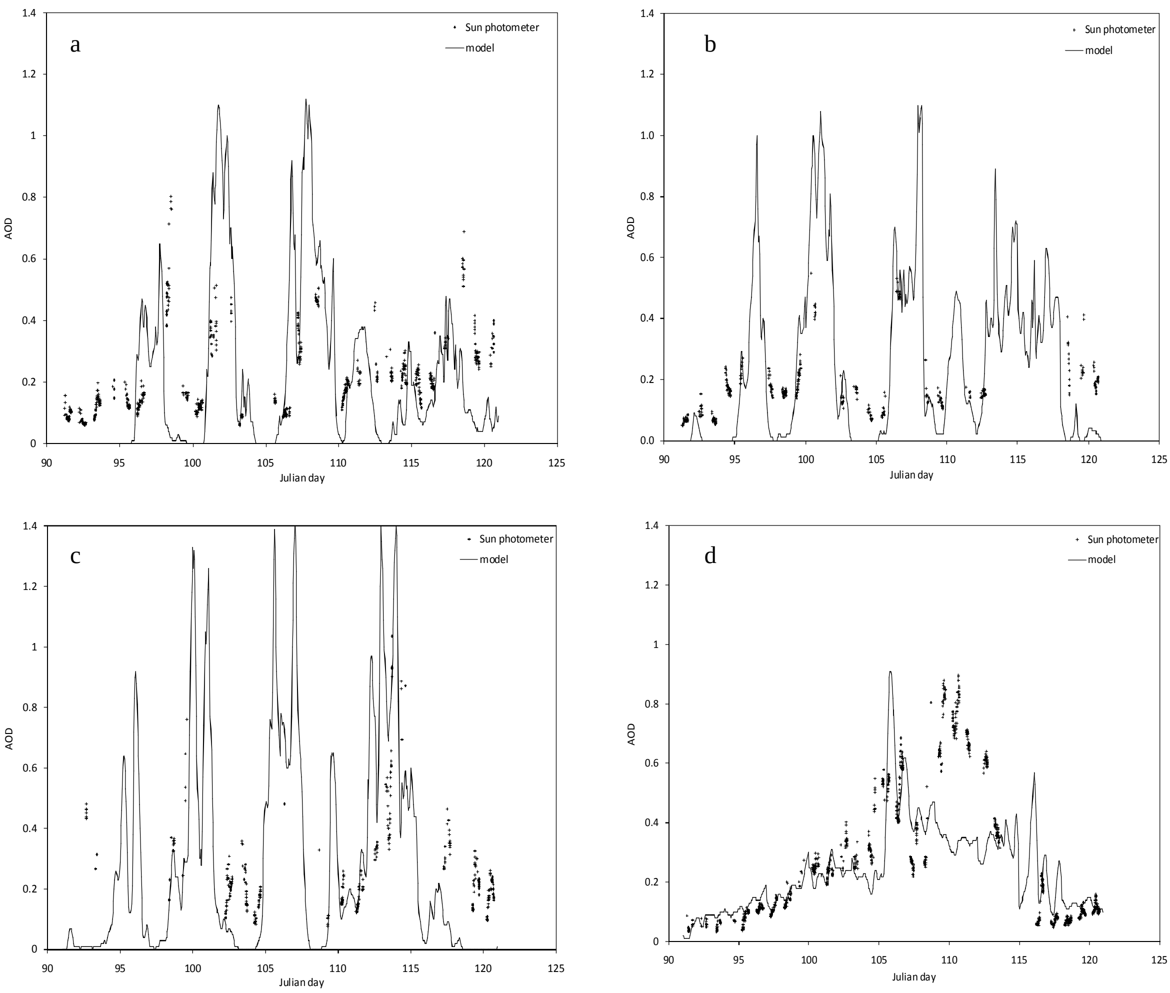


Figure 11: Observed and modeled time-series of the interpolated AOD at 532 nm for April 2006 at a) Crete, b) Lampedusa, c) Blida and d) Tamanrasset.

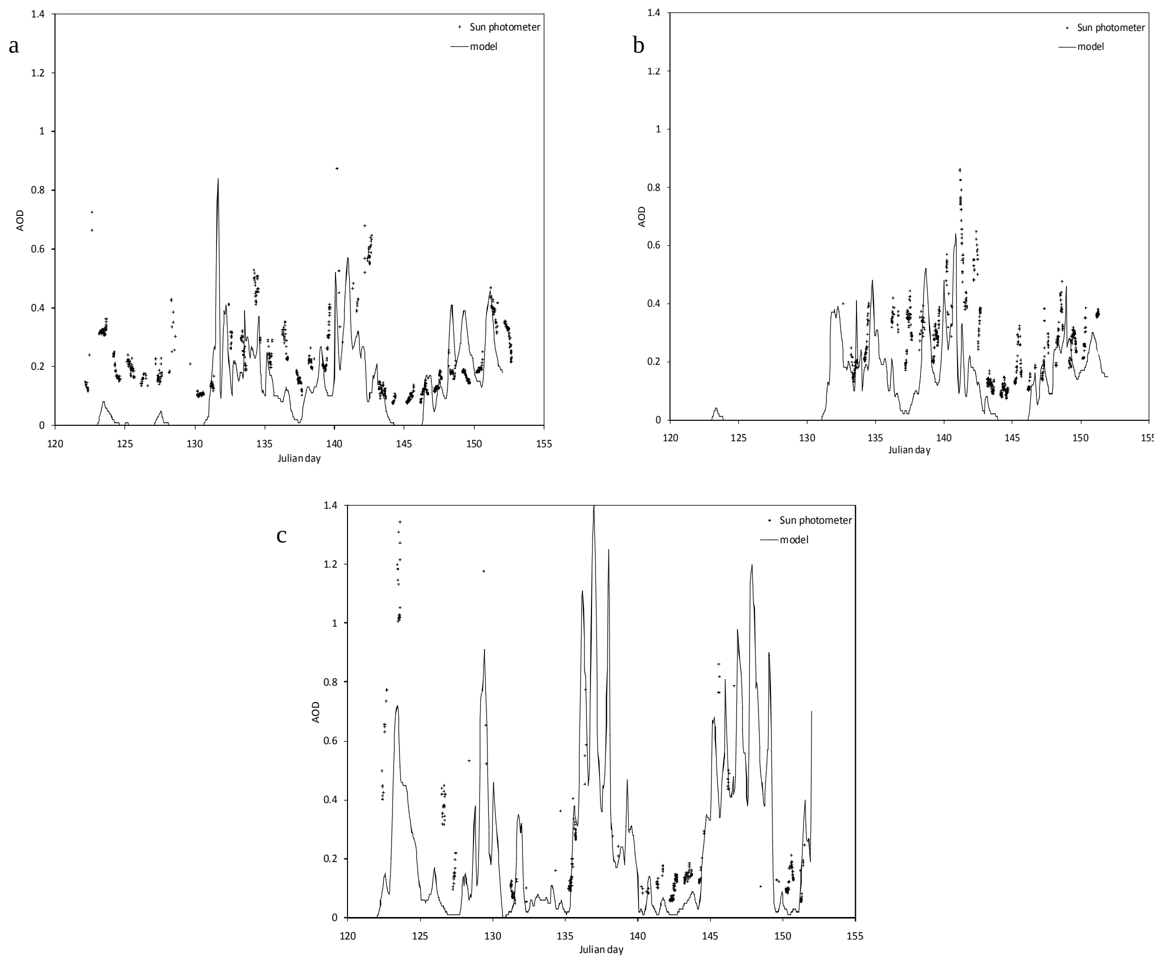


Figure 12: Observed and modeled time-series of the interpolated AOD at 532 nm for May 2008 at a) Crete, b) Athens and c) Blida.

## 4.5 RAMS/ICLAMS dust evaluation

The Regional Atmospheric Modeling System (RAMSv6) (Cotton et al., 2003) is the core model used for the development of the Integrated Community Limited Area Modeling System (RAMS/ICLAMS) (Solomos et al., 2011). RAMS/ICLAMS is a fully coupled integrated meteorology-chemistry modelling system that is developed as a forecasting and research tool for process studies, air pollution and regional climate applications. The online approach is applied, with the method of a single modelling core, to all processes that influence pollutant transport and transformation, chemistry ï microphysical interactions and the direct and indirect feedbacks of gas and aerosol pollutants on the heating rates and photolysis rates, cloud properties and precipitation. Solomos et al., (2011) used this modelling system to assess the impact of mineral dust and sea salt on several meteorological processes, such as cloud development and precipitation patterns. The air quality submodel considers emissions, photodissociation reactions, gas and aqueous phase chemical transformations, aerosol processes, aerosol-radiation-cloud interactions and removal mechanisms.

The saltation and bombardment approach as described in Marticorena et al., (1995) us used for the parameterization of dust emissions. The dust scheme utilizes eight bins for the dust transport size distribution with effective radius of 0.15, 0.25, 0.45, 0.78, 1.3, 2.2, 3.8 and 7.1 εm (Perez et al., 2006, Spyrou et al., 2010). Dust particles are not chemically speciated in the model. Sea salt emissions are performed at two size bins, namely accumulation and coarse, following the open sea white - cap formation

(Monahan et al., 1986; Gong, 2003; Zhang et al., 2005) The coastline sea salt flux parameterization is described in Leeuw et al. (2000). The photochemical scheme uses the basic formulations proposed by Madronich et al. (1987). The dry deposition module follows the resistance model of Wesely (1989). The gas phase chemistry module is based on the chemistry mechanism of the Statewide Air Pollution Research Center, Version 1999 - SAPRC99 (Carter et al., 2000, 2003). The aqueous chemistry sub-module calculates the changes in pollutant concentrations that result from the interaction of gases with droplets (Walcek and Taylor, 1986). The computation of the aerosol CCN activation is performed explicitly as described in the work of Nenes and Seinfeld, (2003). The formation of ice nuclei (IN) is also calculated online with the scheme of Barahona and Nenes (2009). The aerosol composition is based on the Model-3 Community Multiscale Air Quality (CMAQ) method (Binkowski and Roselle, 2003) and the aerosol treatment is derived from the Regional Particulate Model (RPM) (Binkowski and Shankar, 1995). The aerosol size distribution follows a modal approach with three lognormal distribution modes that include the aitken (D=0.01-0.1εm), the accumulation (D=0.1-2.5εm) and the coarse mode (D> 10εm). The inorganic thermodynamic processes are treated by the ISORROPIA equilibrium model (Nenes et al., 1998) and the formation of the secondary organic aerosol (SOA) is based on the work of Schell et al., (2001). The biogenic emissions are calculated online following the method described in Guenther et al. (1995).

### 4.6 Dust event over Eastern Mediterranean and associated flood

On 29 January 2003, an event of heavy precipitation took place over Northern Israel. The period of interest was characterized by a low pressure system and a dust event over East Mediterranean. The wind field exhibited a prevailing south-westerly flow that leads to an enhanced transport of dust particles over the Israeli coast and Lebanon. Several studies on this event [Levin et al., 2005; Solomos et al., 2011] indicated that the mineral dust and the sea salt particles that penetrated the cloud system provided significant amounts of hygroscopic particles. A considerable fraction of these natural particles was activated as CCN. In these studies, the development of the cloud system and the spatiotemporal features of the precipitation field have been found to be strongly related to the properties of the natural aerosol particles (concentration and chemical composition). During the days of the event MEIDEX measuring campaign was active and aircraft measurements are used for comparison with model results. Additionally measurements from several inland stations are also available.
RAMS/ICLAMS was used to simulate the concentration of the particulate matter in the area and their impact on cloud structure. The model configuration is summarized in Table 1.

Table 1 Model configuration

| Grid number | Grid 1/Grid 2/Grid 3 |
|---|---|
| Horizontal spacing | 12 km / 4 km /1 km |
| Vertical grid points | 32 for all grids |
| Vertical spacing | Starts from 50m above ground and stretching up to 18km with a geometric ratio 1.2 |
| Simulation period | 26-31 January 2003 / 28-29 January 2003 /29 January 2003 |

PM10 measurements over three inland stations on the East Mediterranean coastline (in Israel) showed that on the days of the flood event significant ground concentrations were captured. On 28 January 2003 the maximum concentrations reached 160 εg $m^{-3}$

over Afule and Beer Sheva and 230 over εg m$^{-3}$ Modiin. On the next day, 29 January 2003 higher concentrations were observed reaching 460 εg m$^{-3}$ over Afule, 650 εg m$^{-3}$ over Modiin and 530 εg m$^{-3}$ over Beer Sheva. The model captured the reported abrupt increase in aerosol concentrations during the days of the flood event. The comparison of the spatiotemporal features of the modeled and observed aerosol concentrations showed a satisfactory agreement with correlations varying from 0,866 for Afule station to 0,907 for Modiin.

In situ aircraft observations were performed on the days of the event at various heights inside the dust cloud. Levin et al (2005) provides a detailed description of the measurements, the instruments used and the sampling and averaging techniques. For the comparison of the modeled results with the aircraft observations a collocation of the aircraft measurements with the model grid points was performed using a weighted average from the eight nearest model grid points to the location of the measurement. The comparison of the model particles with the airborne observations revealed a satisfactory agreement with a correlation factor of 0,89 (Figure 14). The model is able to reproduce adequately the intensity of the dust storm that is crucial for the performance of cloud-aerosol sensitivity studies.

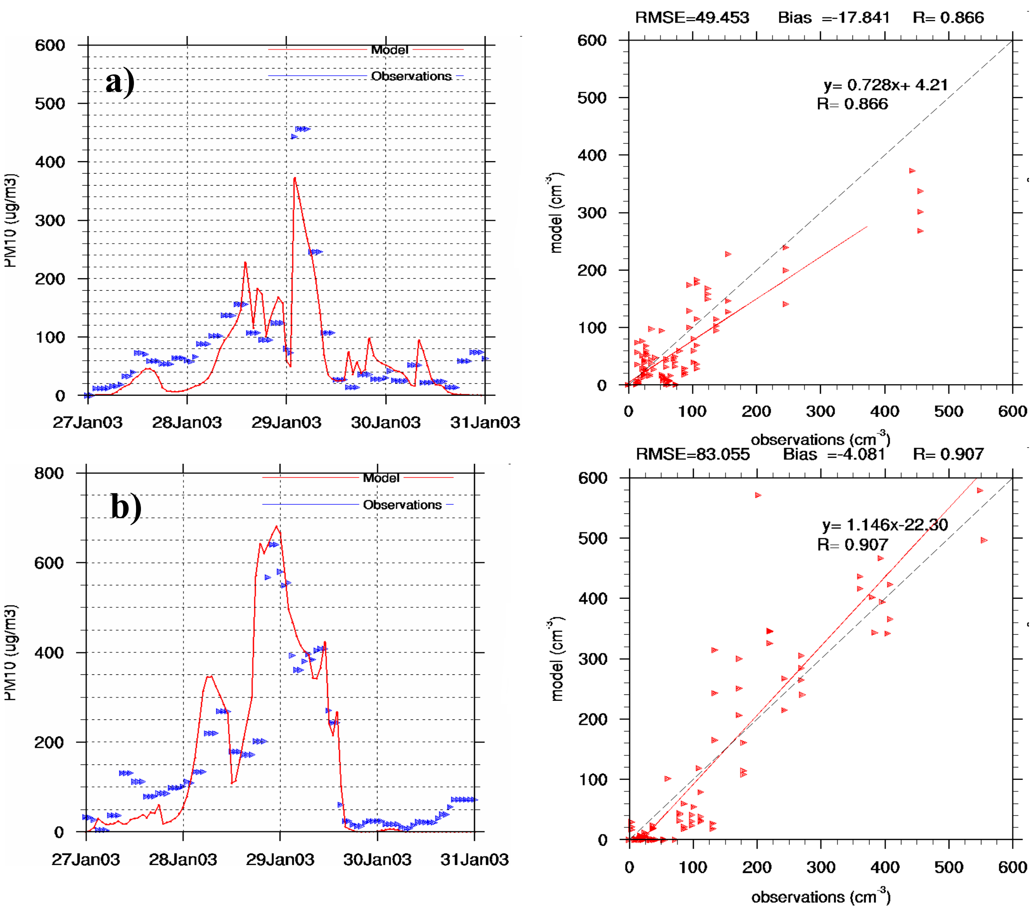

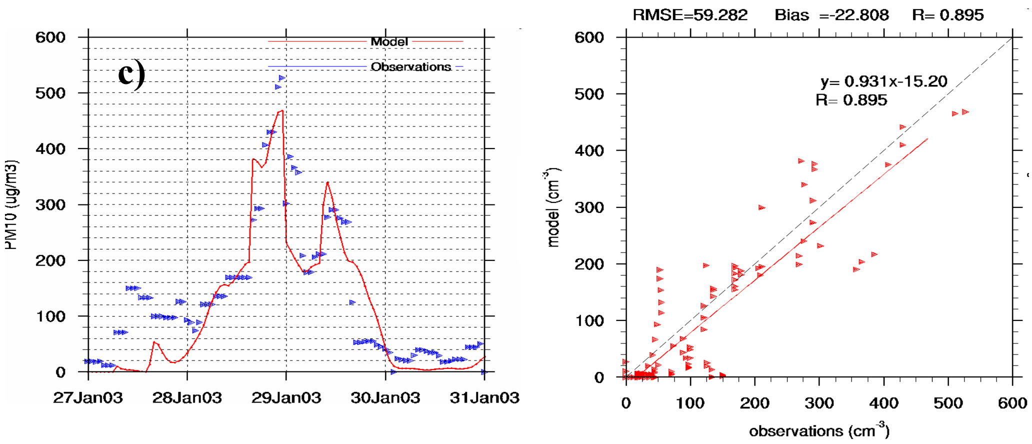


Figure 13 Left plots: Observed (blue crosses) and modeled (red lines) PM10 concentrations (εg m$^{-3}$) over a) Afule, b) Modiin and c) Beer Sheva stations on 27-31 January 2003 and right plots: the respective scatter plots

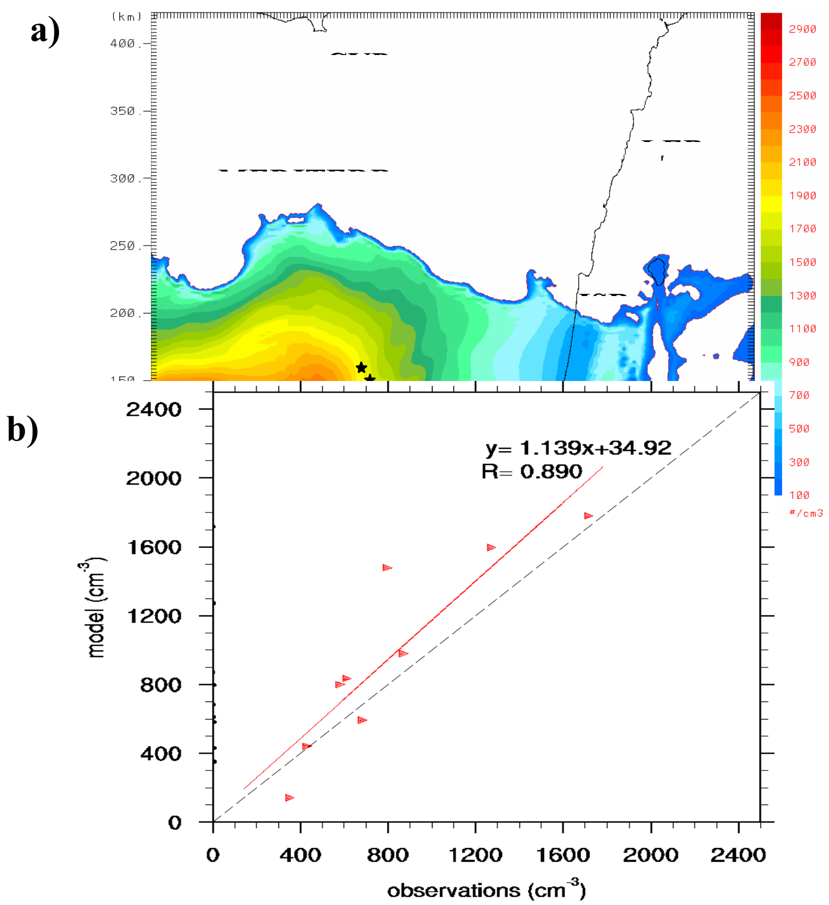


Figure 14 a) Modelled dust number concentration in cm$^{-3}$ at 538 m and aircraft measurement points on 28 January 2003, 09:20 UTC and b) aircraft measurements of natural particles versus modeled dust and sea salt concentrations inside the dust cloud (less than 2 km height). Red line indicates the regression line and black dotted line indicates the $y$ = $x$ line.

### 4.7 Dust mobilization from density currents

During 31 May 2006 a low-pressure system was located over Morocco and southern Spain as shown in Figure 15. During the afternoon hours of 31 May 2006 enhanced convection and intense precipitation was reported over the Atlas mountains due to the trough passage and the existence of cold air at upper levels. These convective clouds produced significant amounts of daily accumulated precipitation that exceeded 30mm over the area south of the Atlas Mountains. At 15:00 UTC, the station of Errachidia (31.93N, 4.40W) reported a thunderstorm (rainfall rate 11 mm $h^{-1}$) that was accompanied by a drop in temperature of about 10$^{o}$C (11-12$^{o}$C at 14:00 UTC). These conditions are favourable for the development of storm downdrafts due to evaporative cooling. Some of the raindrops that fall through a warmer and unsaturated environment evaporate before reaching the ground. Cooler air, caused by the absorption of the vaporization latent heat and the consequent decrease in the ambient temperature, falls to the ground (cool pool).

As described in Solomos et al. (2012) RAMS/ICLAMS was configured using four two-way interactive nesting grids: a coarse 24 km, an intermediate of 4.8 km and two grids of 1.6 km horizontal resolution as illustrated in Figure 15. The vertical coordinates are hybrid terrain following ů$_{z}$, starting with a resolution of 20 m near the ground and stretching up to 18 km with a factor of 1.10. This configuration allows sufficient representation of the vertical tropospheric structure and includes an adequate number of model levels near the ground, in order to resolve the convective and turbulence motions at the lower 3km of the atmosphere. The ECMWF 0.5$^{o}$×0.5$^{o}$ objective analysis fields were used for initial and lateral boundary conditions. The sea surface temperature (SST) is the NCEP 0.5º×0.5º analysis data. The Kain-Fritsch (Kain and Fritsch, 1993) convective parameterization scheme was activated for the outer grid and the RRTMG radiative transfer scheme (*Mlawer et al.,* 1997; *Iacono et al.,* 2000) was used for both sortwave and longwave bands on all grids. For the intermediate and finest model grids no convective parameterization was used and convection was resolved only by the explicit microphysics scheme of the model.

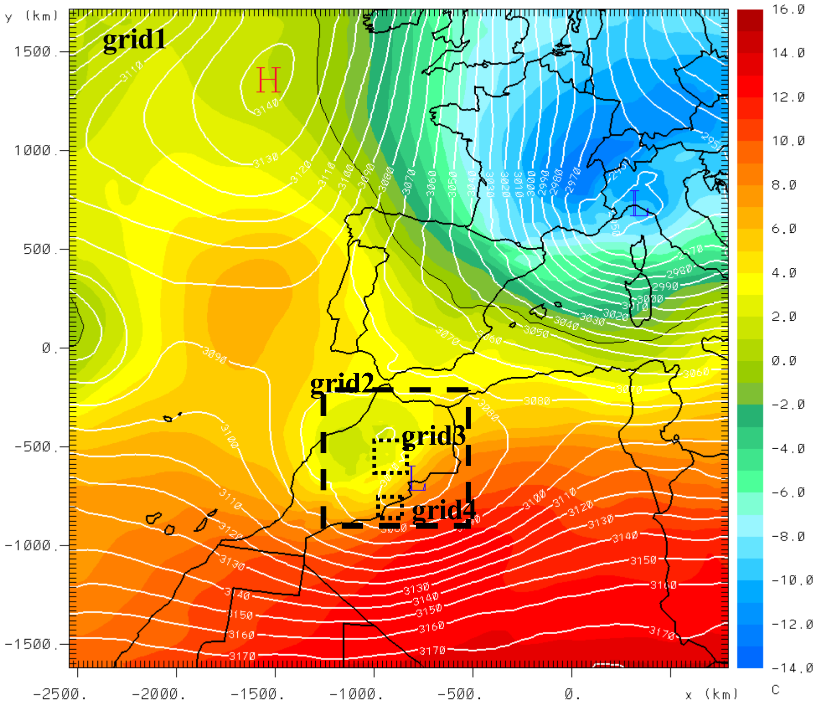


The formation of a cool pool south of the Atlas Mountains leaded to the development of a fast propagating density current. The steep topographic slope enhanced propagation.

The system moved southwards towards the Morocco-Algeria borderline accompanied by dust production and by a squall line of shallow convective clouds as seen in Figure 16. Modeling output was compared to satellite observations from the Meteosat Second Generation (MSG) Spinning Enhanced Visible and InfraRed Imager (SEVIRI) (Schmetz et al., 2002). These images are available online by EUMETSAT (http: //www.eumetsat.int). Both model results and satellite observations from the MSG/SEVIRI dust indicator system showed an extended frontal line of about 300 km that was associated with intense dust production and cloud cover. As shown in Solomos et al (2012) the capability of the model to reproduce adequately the abrupt changes in the meteorological conditions is crucial to the representation of the feature of the density current. RAMS/ICLAMS captured satisfactorily the spatiotemporal characteristics of the dust mobilization.

Figure 15 Geopotential height (white contour lines every 10 gpm) and temperature at 700 hPa (colour palette in °C) - 11:00 UTC on 31 May 2006. The dashed rectangulars indicate the locations of the nested grids.

Another region where significant interaction between mesoscale atmospheric features and dust mobilization has been observed is the sub-Saharan Sahel zone (i.e. *Bou Karam et al*., 2009). The north disposal of the Intertropical Convergence Zone (ITCZ) during the summer period allows the establishment of a SW monsoon flow at lower atmospheric levels over the Sahel area. This kind of flow is usually associated with moisture convergence and development of convective clouds. The outflow boundaries that are generated from these convective storms allow the advection of dust towards north directions. These dust particles penetrate the transient zone between monsoon flow and the easterly trade winds (i.e. harmattan wind) and intersect with dust plumes at the north boundary of the discontinuity zone.

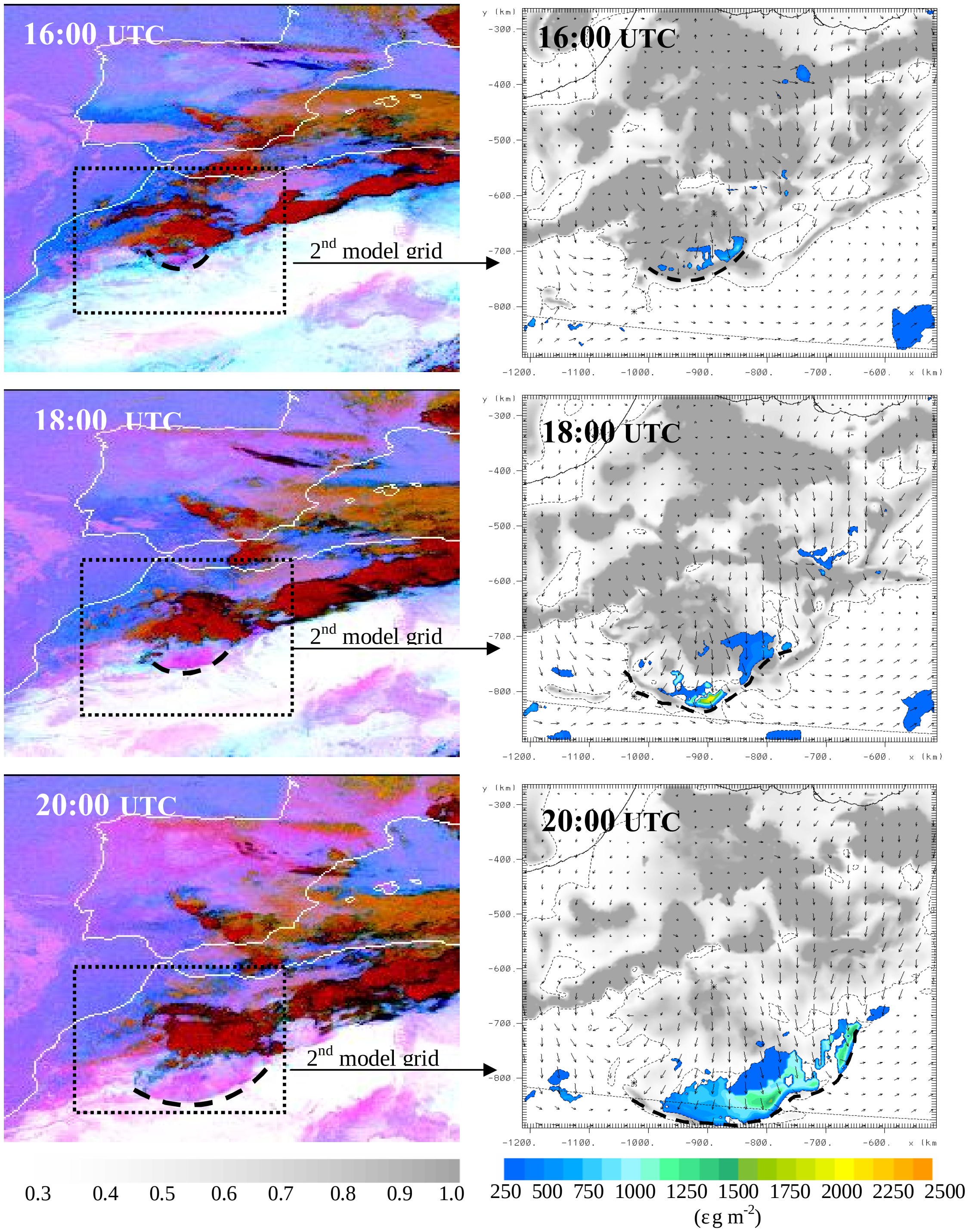


Figure 16 Left column: MSG/SEVIRI dust indicator satellite images over North West Africa. Dark red colors indicate clouds and purple colors indicate desert dust. Right column: Corresponding model cloud fraction (grayscale) and dust production flux (colour palette in εg $m^{-2}$). The leading edge of the propagating density current is denoted with black dashed lines.

Such an example is illustrated in the satellite image of 14 July 2003, 02:00 UTC that is exhibited in Figure17a. In this image, dark red colors represent cloud formations while dust particles are shown in purple. The location of a dust plume over Algeria and Mali borderline is indicated by the black dashed line. In order to investigate the atmospheric conditions and the origin of dust particles during this case, the model was set up with two grids as seen in Figure 17b: A coarse grid of 24×24 km covering most of the western Africa and part of eastern Atlantic and a second nested grid of 6×6 km resolution that was placed over Algeria-Mali border. Initial and boundary conditions were taken from the ECMWF 0.5$^{o}$×0.5$^{o}$ objective analysis fields and sea surface temperature was from the NCEP 0.5º×0.5º analysis data. The online dust production ï transportation ï deposition module was enabled and the vertical model structure was the same as described in section three.

Model results for the 13$^{th}$ July 2003 indicated a northern displacement of the ITCZ that was located over Sahel at about 18-21° N as seen in Figure 17b. The location of the ITCZ is identified by the discontinuity in wind field that separates the SW monsoon flow from the NE trade wind. The strong NE winds that dominated across the Western Saharan coastline were responsible for the mobilization of dust at this area. These particles were transported towards the Atlantic Ocean as indicated by the red isopleths of dust-load over Western Africa coast in Figure 17c. Also, channeling of the NE dry harmattan flow over the Hoggar Mountains was responsible for significant dust production at this area. South of the ITCZ, the Western African monsoon flow at lower tropospheric levels is transferring moist air from the Atlantic Ocean towards Mali and Niger. The depth of the monsoon flow was about 1.5 km during the simulation period. Above this height, the atmospheric circulation was dominated by the African easterly jet.

The western monsoon flow behaves in a way similar to density current formations and is associated with the development of Mesoscale Convective Systems (MCS) as discussed in *Bou Karam et al.* (2008). The outflow boundaries that were generated from these MCS enforced the western flow at lower atmospheric levels. In Figure 17c, a ridge of moist monsoon air is obvious at 925 mb height across the Algerian-Mali borderline and the discontinuity zone boundary has been displaced to the north. The dust particles at this area were transferred northwards and as seen in Figure 17c the dustload over Algeria territory reached 1750 mg m$^{-2}$ at 02:00 UTC on 14 July 2003. The cold and moist monsoon air in Figure 17d wedges below the warmer NE air similar to the density current formations that were described in previous sections. Increased dust concentrations at the northern part of the domain in Figure 17d as well as the sharp gradient in dust concentration that is obvious along the interface between monsoon and harmattan flow is indicative of the role of such processes for dust transportation in this area.

Another such event took place on 4 August 2006. During the midday of August, 3 2006 the prevailing SW monsoon flow over Mali at the lower tropospheric levels (below 1.5 km) resulted in low level convergence along the discontinuity zone. Convective clouds were developed in the area and the associated evaporation cooling near the surface resulted in the generation of an outflow boundary and the mobilization of dust particles as seen in Figure 18a. The model configuration was similar to the previous case and a 6×6 km nested grid was applied over Mali-Algerian border as indicated in Figure 18b. The north-propagating dust front is identified in Figure 18b by the red dustload contours. The vertically integrated concentration of dust particles reached 1700 mg m$^{-2}$ at 02:00 on 4 august 2006 when the system entrained the ITCZ. Above 1.5 km height the flow pattern was dominated by a northeasterly jet that transported the convective clouds towards southwest. These clouds continued precipitating and produced a secondary non-dust productive outflow front that is indicated by the dashed red line in Figure 18b.

A similar dust episode can be identified in the satellite image of Figure 18c. The convectively driven dust storm in this case was triggered at the area of South Sudan in eastern African coast. The model was applied with a two grid configuration similar to the previous cases and the location of the nested 6×6 km grid is indicated in Figure 18d. The development of convective clouds over South Sudan on the afternoon hours of 29 April 2007 and the associated rainfall cooling was responsible for the generation of a northward propagating density current. This system was accompanied by dust production that is characteristic of the ñhaboobsò at this area. As seen in Figure 18d, dustload concentrations of up to 600 mg m$^{-2}$ were found over central Sudan south of the ITCZ at 22:00 UTC.

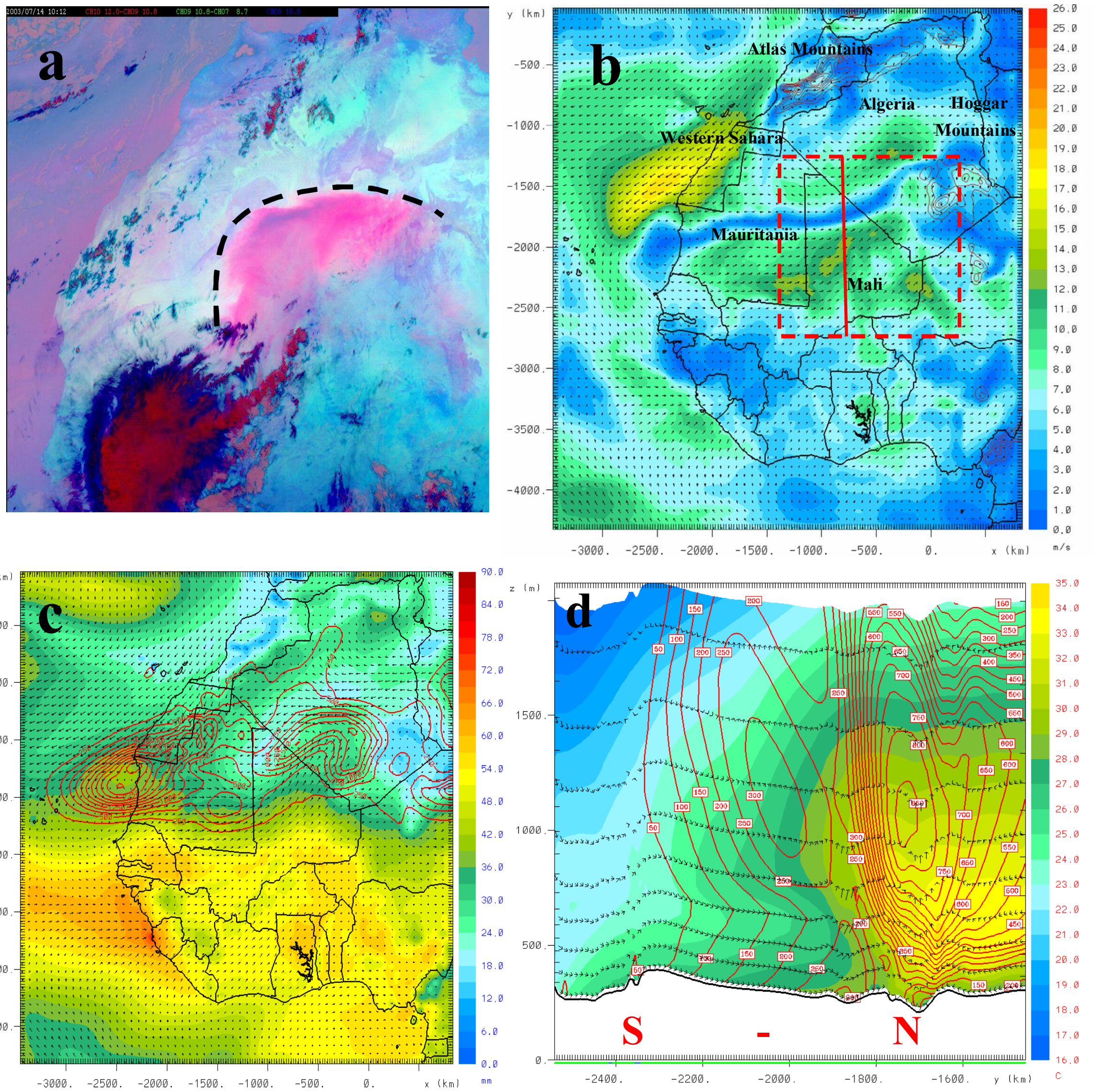


Figure 17: a)MSG/SEVIRI instrument satellite image over West Africa on 14 July 2003 02:00 UTC. Dark red colors indicate Mesoscale Convective System clouds (MCS) and light purple colors indicate desert dust. The black dashed lines denote the location of the desert dust front. b). Wind speed at 925 mb (color palette), and topography contours (brown contour lines from 1000 to 2750 by 250) at 13 July 2003, 12:00 UTC. The red dashed rectangular indicates the location of the nested model grid. The solid red line indicates the location of the cross-section for Figure 17d. c) Vertically integrated water (color palette in mm) and integrated column dust (dustload) contours (from 250 to 3000 mg m$^{-2}$ every 250 mg m$^{-2}$) at 925 mb at 14 July 2003, 02:00 UTC. The moist monsoon air penetrates the discontinuity zone near Algerian ï Mali borderline and the dust particles at this area are transferred towards central and north Algeria. d) Vertical cross-section of temperature (color palette in °C) and dust concentration (red contour lines in εg m$^{-3}$). Intrusion of the colder monsoon air transports dust particles towards the north part of Algeria.

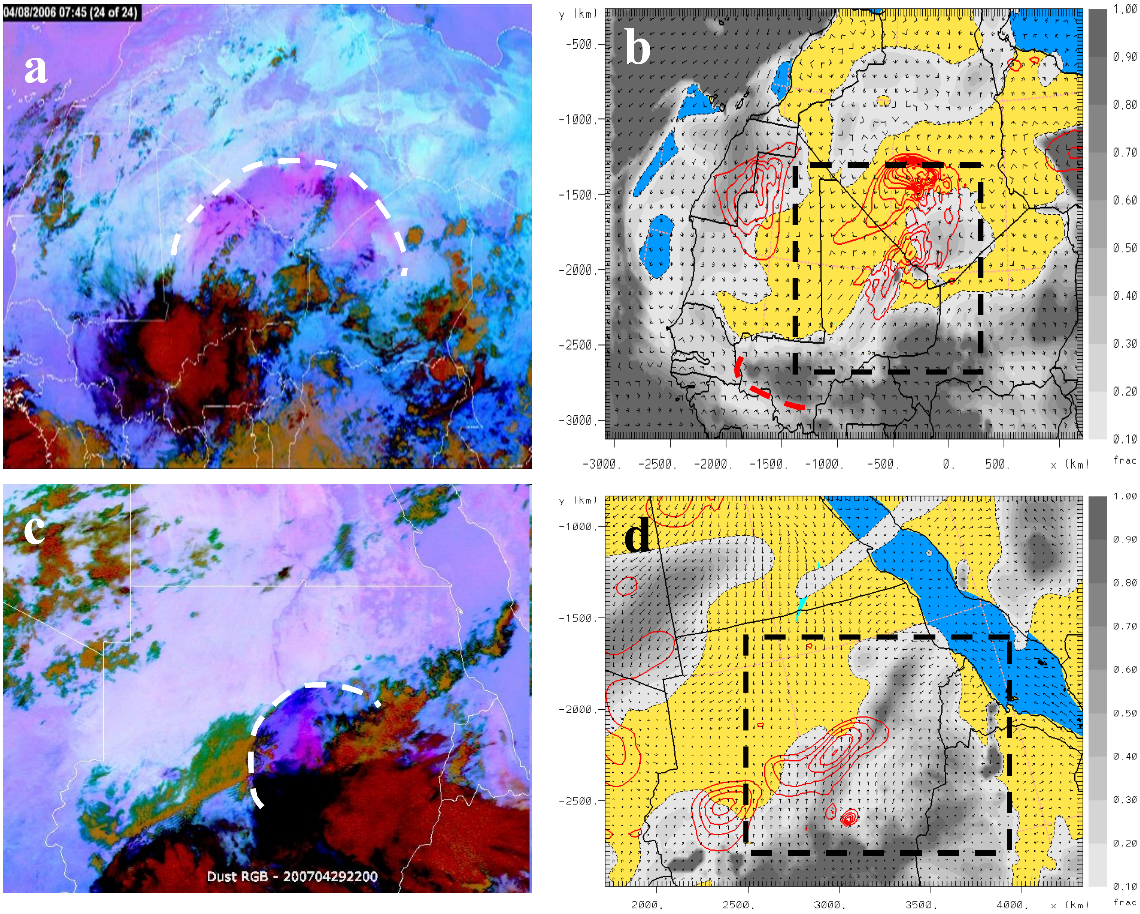


Figure 18: a) MSG/SEVIRI instrument satellite image over West Africa on 4 August 2006 07:45 UTC. Dark red colors indicate Mesoscale Convective System clouds (MCS) and light purple colors indicate desert dust. The white dashed line denotes the location of the desert dust front. b) Zoom from the outer model grid: Cloud cover (greyscale), dust-load (red contours every 150 mg $m^{-2}$) and wind arrows at $1^{st}$ model layer (19.5 m) on 4 August 2006 02:00 UTC. The black dashed rectangle indicates the location of the nested 6×6 km grid and the red dashed line indicates the location of a secondary SW propagating outflow. c) MSG/SEVIRI instrument satellite image over Sudan on 29 April 2007 22:00 UTC. Dark red colors represent Mesoscale Convective System clouds (MCS) and light purple colors indicate desert dust. The white dashed line denotes the location of the desert dust front. d) Zoom from the outer model grid: Cloud cover (greyscale) and dust-load (red contours every 100 mg $m^{-2}$) at 22:00 UTC. The dashed rectangular indicates the location of the 6×6 km nested grid.

## 5. Other evaluation initiatives

### 5.1. The MACC-II evaluation

Monitoring Atmospheric Composition and Climate (MACC-II) is the current pre-operational atmospheric service of the European Global Monitoring for Environment and Security (GMES) program. MACC-II uses a comprehensive global monitoring and forecasting system, which includes the analysis/assimilation? of MODIS aerosol optical depth data, to provide daily 5-day forecast.

The DOD at 550 nm forecast by the MACC-II model (Benedetti et al., 2009; Morcrette et al., 2009), as well as the contributions of other aerosol types, are drawn together with the AERONET and MODIS retrievals of AOD in monthly charts for selected stations. However, the scoring metrics that are calculated on a monthly-averaged time frame for different regions or stations are always calculated for the total atmospheric aerosol, without any distinction of the species. This evaluation is complemented with regular reports describing the model performance to forecast major and recent events (available online at www.gmes-atmosphere.eu).

As part of the evaluation, a large effort has been devoted to the investigation of how to best use ground-based measurements, such as AERONET, to assess the models in data-scarce regions. Calculating scores is complicated by the geographical inhomogeneity of the observation sites, so any change in the geographical spread of the sites over time may lead to changes in the scores. Therefore, long-term time-series of the scores could then reflect changes in the observing system rather than changes in forecast quality, which is not the objective. In order to reduce geographical bias and increase long-term stability model-versus-AERONET scores are computed using weights for each observation that reflect the local observation density at each observation time.

### 5.2. Models evaluation at the BSC-CNS

The BSC-CNS daily run the DREAM model and then replaced it by the BSC-DREAM8b. These models have been used for dust forecasting and as dust research tools in North Africa and the Mediterranean (e.g. Amiridis et al., 2009; Klein et al., 2010; Pay et al., 2010; Alonso-Pérez et al., 2011).

The BSC-DREAM8b model is daily evaluated using NRT observations including AERONET data and satellite products from MODIS and METEOSAT Second Generation: https://www.bsc.es/earth-sciences/mineral-dust/bsc-dream8b-forecast/nrt-evaluation Figure 7 shows how the model reproduces the dust plumes over West Chad and Iraq as well as the dust transport over the tropical Eastern Atlantic

Several case studies have outlined the good skills of DREAM (e.g. Balis et al., 2006; Kishcha et al., 2007) and BSC-DREAM8b (e.g. Pérez et al., 2006a, b; Papanastasiou et al., 2010) concerning both the horizontal and vertical extent of the dust plume in the Mediterranean Basin. The model has also been validated and tested over longer time periods in the European region (e.g. Basart et al., 2012; Pay et al., 2012) and against measurements at source regions, using data from the Saharan Mineral Dust Experiment (SAMUM-I) (Haustein et al., 2009) and the Bodélé Dust Experiment (BODEX) (Todd et al., 2008).

The BSC-CNS also runs the NMMB/BSC-Dust model. Pérez et al. (2011) evaluated it at regional and global scales. At a global scale, the model lies within the top range of those involved in the Aerosol inter-comparison project (AeroCom, http://aerocom.met.no) in terms of performance statistics for surface concentration, dust deposition and DOD. At regional scale, the model has shown a significant skill in reproducing the daily variability and seasonal spatial distribution of DOD over Northern Africa, Middle East and Europe. Haustein et al. (2012) evaluated the model over source regions using data from the SAMUM I and BODEX campaigns.

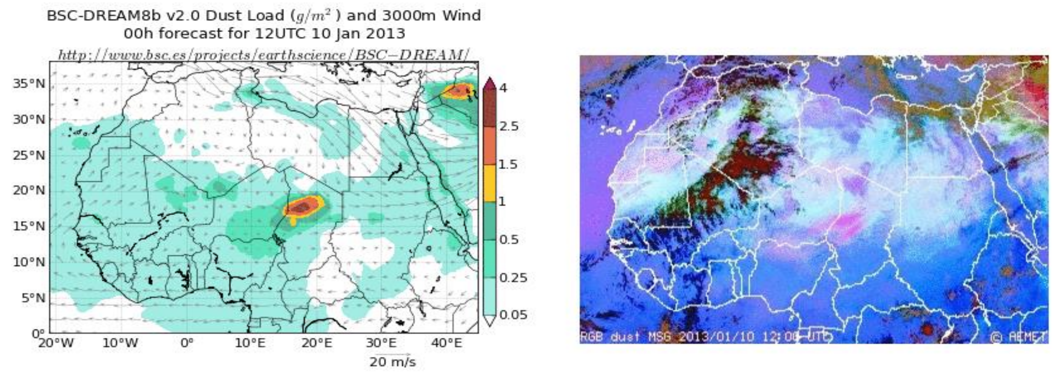


Fig. 7: The BSC-DREAM8b dust load forecast for 10 Jan 2012 at 12:00 (left) shows a good agreement with the EUMETSAT RGB-Dust product based on Meteosat Second Generation.

### 5.3. Case study evaluation

Multiple case studies concerning a single model can be found in the literature (e.g. Perez et al., 2006; Heinold et al., 2007; Cavazos et al, 2009). On the other hand, inter-comparisons of multiple models simulating the same event are described by Uno et al. (2006) and Todd et al. (2008). The former compared multiple regional dust models over Asia, while the latter compared five regional models for a 3-day dust event over the Bodélé depression. Both studies reveal the ability of models to reproduce the onset and duration, but not the magnitude of a given dust event. Finally, intercomparisons can also be conducted to assess the model performance to predict a given event. Shao et al. (2003) analyzed a real-time prediction system of dust storms in Northeast Asia. This forecast system successfully predicted the temporal and spatial evolution of the dust plume being analyzed. Within the SDS-WAS NAMEE node, the first comprehensive intercomparison of dust forecast models is been conducted to examine the predictability of dust transport from Northern Africa to Europe. Four state-of-the-art dust forecast models are analyzed in their ability to predict an intense Saharan dust outbreak transporting dust over Western Europe up to Scandinavia between 5$^{th}$ and 11$^{th}$ April 2011. Each model is compared against a set of different observations, namely surface concentration, aerosol optical depth (AOD), lidar profiles, wind at 10m and wind profiles. In addition, the meteorological fields associated to the dust outbreak and transport of each model is compared to reanalysis fields. The comprehensive inter-comparison of the models will reveal strengths and weaknesses of individual forecasts and provide an assessment of uncertainties in simulating the atmospheric dust cycle. Studying a single dust event allows to investigate the capacity of the models to predict the approach of a dust event with a higher temporal resolution of a few hours.

Inter-comparison studies are not necessarily limited to a single event. They can analyze the models performance to simulate the dust cycle during an extended time period. A broad inter-comparison of 15 global aerosol models was conducted within the framework of the aerosol inter-comparison project, AeroCom (Huneeus et al., 2011). Each model was compared to observations of total AOD, dust deposition, Ängström exponent, coarse mode fraction AOD and dust surface concentrations. The study revealed a generalized better skill to simulate vertically-integrated variables, such as AOD, than dust concentration at the surface.

## 6. Dust parameterizations in air quality forecasting systems

During recent years, several countries have implemented air quality forecasting systems (AQFS) to issue predictions of particulate matter and gaseous pollutants aimed to take action to prevent or reduce adverse effects. Initially, these systems only considered anthropogenic emissions and it was found that chemical transport models recursively underestimated the aerosol concentrations over specific areas. In regions such as southern Europe, the existence of extensive semi-arid soils and the frequent occurrence of desert dust outbreaks forced to consider natural emissions in the simulations. Incorporating dust parameterizations has significantly improved the evaluation results of some AQFS. This is the case of the BSC-DREAM8b model integrated into the CALIOPE AQFS (Jiménez-Guerrero et al., 2008; Pay et al., 2012) and the DREAM model coupled with the Transport Chemical Aerosol Model (Carnevale et al., 2012).

## 6. Conclusions

Dust forecast models can provide useful information to forecasters. They may reproduce the key features of large dust plumes, especially with regards to its spatial extent. Its skill is lower to provide quantitative values. Models perform better in simulating the evolution of vertically integrated parameters such as DOD than deposition or surface concentration. Finally, they suffer to reproduce small-scale events such as those associated to mesoscale thunderstorm downdrafts (Knippertz et al., 2007; Miller et al., 2008) or to micro-scale events such as those related to breaking of the nocturnal low-level jet (Abdou et al., 2010; Knippertz and Todd, 2010).Dust prediction is also limited by the scarcity of observations available for data assimilation and model evaluation (Huneeus et al., 2011).

## 7. References

Abdou, K., D. J. Parker, B. Brooks, N. Kalthoff, and T. Lebel, 2010: The diurnal cycle of lower boundary-layer wind in the West African monsoon. Quat. J. Royal. Meteor. Soc., 136: 66ï 76. doi: 10.1002/qj.536

Alonso-Perez S., E. Cuevas, C. Perez, X. Querol, J.M. Baldasano, and R. Draxler, 2011: Positive Trends Of African Air mass Intrusions Over The Subtropical Eastern North Atlantic Ocean In Winter. Tellus B, 63B: 255-265 doi: 10.1111/j.1600-0889.2010.00524.x

Amiridis V., M. Kafatos, C. Perez, S. Kazadzis, E. Gerasopoulos, and co-authors, 2009: The potential of the synergistic use of passive and active remote sensing measurements for the validation of a regional dust model. Ann. Geophys. 27, 3155-3164.

Anderson, J.R, Hardy, E. E., Roach, J. T. and Witmer R. E. 1976: A Land Use And Land Cover Classification System For Use With Remote Sensor Data, Geological Survey Professional Paper 964.

Balis D., V. Amiridis, S. Kazadzis, A. Papayannis, G. Tsaknakis, S. Tzortzakis, N. Kalivitis, M. Vrekoussis, M. Kanakidou, N. Mihalopoulos, G. Chourdarkis, S. Nickovic, C. Pérez, J. M. Baldasano, and M. Drakakis, 2006: Optical characteristics of desert dust over the East Mediterranean during summer: a case study. Ann. Geophys, 24: 807-821.

Barahona, D. and A. Nenes, 2009: Parameterizing the Competition between Homogeneous and Heterogeneous Freezing in Ice Cloud Formation - Polydisperse Ice Nuclei, Atmos.Chem.Phys., 9, 5933-5948.

Basart, S., C. Pérez, S. Nickovic, E. Cuevas, and J. M. Baldasano, 2012: Development and evaluation of the BSC-DREAM8b dust regional model over Northern Africa, the Mediterranean and the Middle East. Tellus Series B - Chemical and Physical Meteorology 64, 1-23

Ben Mohamed, A., J. P. Frangi, J. Fontan, and A. Druilhet, 1992: Spatial and temporal variations of atmospheric turbidity and related parameters in Niger. J. Appl. Meteor. 31, 1286ï 1294.
Benedetti, A., J.-J. Morcrette, O. Boucher, A. Dethof, R. J. Engelen, M. Fisher, H. Flenthe, N. Huneeus, L. Jones, J. W. Kaiser, S. Kinne, A. Mangold, M. Razinger, A. J. Simmons, and M. Suttie, 2009: Aerosol analysis and forecast in the ECMWF Integrated Forecast System: Data assimilation. J. Geophys. Res., 114, D13205, doi:10.1020/2008JD011115.
Betts, A.K., and M. J. Miller, 1986: A new convective adjustment scheme. Part II: Single column tests using GATE wave, BOMEX, and arctic air-mass data sets. Quart. J. Roy. Meteor. Soc., 112, 693-709.
Binkowski, F.S. and Shankar U. 1995 : The regional particulate matter model, 1. model description and preliminary results, Journal of Geophysical research, 100, 26191-26209.
Bou Karam, D., C. Flamant, P. Knippertz, O. Reitebuch, J. Pelon, M. Chong, A. Dabas , 2008: Dust emissions over the Sahel associated with the West African Monsoon inter-tropical discontinuity region: a representative case study, *Q. J. R. Meteorol. Soc.* 134: 621ï 634.
Bou Karam, D., C. Flamant, P. Tulet, J.-P. Chaboureau, A. Dabas, and M. C. Todd, 2009: Estimate of Sahelian dust emissions in the intertropical discontinuity region of the West African Monsoon, *J. Geophys. Res.*, 114, D13106, doi:10.1029/2008JD011444.
Carnevale, C., G. Finzi, E. Pisoni, M. Volta, P. Kishcha, and P. Alpert, 2008: Integrating Saharan dust forecasts into a regional chemical transport model, 2012: A case study over Northern Italy. Science of the Total Environment, 417ï 418 (2012) 224ï 231
Carter, W.P.L.: Implementation of the SAPRC-99 chemical mechanism into the models-3 framework. Report to the United States Environmental Protection Agency, 2000.
Carter, W. P. L., Sauer, C.G., Fitz, D.R., Bumiller, K., Bufalino, C., Malkina, I., Pisano, J.T., Smith, M. and Cocker, D.R III: A New Environmental Chamber Facility for Atmospheric Chemical Mechanism Evaluation, Presented at the Gordon Conference on Atmospheric Chemistry, Big Sky Resort, Montana, September 7-12, 2003.
Cavazos, C., M. C. Todd, and K. Schepanski, 2009: Numerical model simulation of the Saharan dust event of 6ï 11 March 2006 using the Regional Climate Model version 3 (RegCM3). J. Geophys. Res., 114, D12109, doi: 10.1029/2008JD011078.
Cotton W. R., and co-authors, 2003: RAMS 2001: Current status and future directions. *Meteoro. and Atmos Phys 82, 5-29.*
D`Almeida, G.A.,: Desert aerosol characteristics and effects on climate. In: Leinen, M., Sarnthein, M. (Eds.), 1987: Palaeoclimatology and Palaeometeorology: Modern and Past Patterns of Global atmospheric transport. NATO ASI series, C, 282, 311-338.
d'Almeida, G. A., 1987: On the variability of desert aerosol radiative characteristics. J. Geophys. Res., 92, 3017-3026
Dubovik, O. and M. D. King, 2000: A flexible inversion algorithm for retrieval of aerosol optical properties from Sun and sky radiance measurements. J. Geophys. Res., 105, 20673-20696.
Ginoux, P., D. Garbuzov, and H. C. Hsu, 2010: Identification of anthropogenic and natural dust sources using MODIS Deep Blue level 2 data. J. Geophys. Res., 115, D05204, doi:10.1029/2009JD012398.
Ginoux, P., J. M. Prospero, T. E. Gill, N. C. Hsu, and M. Zhao, 2012: Global-scale attribution of anthropogenic and natural dust sources and their emission rates

based on MODIS Deep Blue aerosol products. Rev. Geophys., 50, 3, RG3005, doi:10.1029/2012RG000388.
Gong, S. L., 2003: A parameterization of sea-salt aerosol source function for sub- and super-micron particles, Global Biogeochem. Cy., 17, 1097, doi:10.1029/2003GB002079.
Guenther, A., Hewitt, C.N., Erickson, D., Fall, R., Geron, C., Graedel, T., Harley, P., Klinger, L., Lerdau, M., Mckay, W.A., Pierce, T., Scholes, B., Steinbrecher, R., Tallamraju, R., Taylor, J., Zimmerman, P., 1995 : A global model of natural volatile organic compound emissions, Journal of Geophysical Research 100 (D5), pp. 8873ï 8892.
Haustein K., C. Pérez, J. M. Baldasano, D. Müller, M. Tesche, and co-authors, 2009: Regional dust model performance during SAMUM 2006. Geophys. Res. Letters, 36, L03812.
Haustein, K., C. Pérez, J. M. Baldasano, O. Jorba, S. Basart, R. L. Miller, Z. Janjic, T. Black, S. Nickovic, M. C. Todd, R. Washington, D. Müller, M. Tesche, B. Weinzierl, M. Esselborn, and A. Schladitz, 2012: Atmospheric dust modeling from meso to global scales with the online NMMB/BSC-Dust model - Part 2: Experimental campaigns in Northern Africa. Atmos. Chem. Phys., 12, 2933-2958, doi:10.5194/acp-12-2933-2012
Heinold, B., J. Helmert, O. Hellmuth, R. Wolke, A. Ansmann, B. Marticorena, B. Laurent, and I. Tegen, 2007: Regional modeling of Saharan dust events using LM-MUSCAT: Model description and case studies. J. Geophys. Res., 112, D11204, doi:10.1029/2006JD007443.
Hilton, F, and Coauthors, 2012: Hyper spectral earth observation from IASI: five years of accomplishments. Bull. Amer. Meteor. Soc., 93, 347ï 370. doi: http://dx.doi.org/10.1175/BAMS-D-11-00027.1
Holben, B. N., T. F. Eck, I. Slutsker, D. Tanré, J. P. Buis, A. Setzer, E. Vermote, J. A. Reagan, Y. Kaufman, T. Nakajima, F. Lavenu, I. Jankowiak, and A. Smirnov, 1998: AERONET - A federated instrument network and data archive for aerosol characterization. Rem. Sens. Environ., 66, 1-16.
Hsu, N. C., S.-C. Tsay, M. King, and J. R. Herman, 2006: Deep Blue retrievals of Asian aerosol properties during ACE-Asia. IEEE Trans. Geosci. Remote Sens., 44, 3180-3195.
Huneeus, N., M. Schulz, Y. Balkanski, J. Griesfeller, J. Prospero, S. Kinne, S. Bauer, O. Boucher, M. Chin, F. Dentener, T. Diehl, R. Easter, D. Fillmore, S. Ghan, P. Ginoux, A. Grini, L. Horowitz, D. Koch, M. C. Krol, W. Landing, X. Liu, N. Mahowald, R. Miller, J.-J. Morcrette, G. Myhre, J. Penner, J. Perlwitz, P. Stier, T. Takemura, and C. S. Zender, 2011: Global dust model intercomparison in AeroCom phase I. Atmos. Chem. Phys., 11, 7781-7816, doi:10.5194/acp-11-7781-2011.
Iacono, M. J., Mlawer, E. J., Clough, S. A. and Morcrette, J. J., 2000: Impact of an improved longwave radiation model, RRTM, on the energy budget and thermodynamic properties of the NCAR Community Climate Model, CCM3. *J. Geophys. Res.*, 105:14873ï 14890.
Jiménez-Guerrero, P., C. Pérez, O. Jorba, and J. M. Baldasano, 2008: Contribution of Saharan Dust in an Integrated Air Quality System and its On-Line Assessment. Geophys. Res. Letters, 35, L03814, doi: 10.1029/2007GL031580
Kain, J. S. and Fritsch, J.M., 1990 : A one-dimensional entraining/detraining plume model and its application in convective parameterization. J. Atmos. Sci., 47, 2784-2802.
Kallos, G., Nickovic, S., Papadopoulos, A., Jovic, D., Kakaliagou, O., Misirlis, N., Boukas, L., Mimikou, N., Sakellaridis, G., Papageorgiou, J., Anadranistakis, E. and Manousakis, M.: The regional weather forecasting system Skiron: An overview. Proceedings of the Symposium on Regional Weather Prediction on Parallel Computer Environments, 15-17 October 1997, Athens, Greece, 109-122.

Kallos, G., Papadopoulos, A., Katsafados, P., and Nickovic, S., 2006 : Transatlantic Saharan dust transport: Model simulation and results. Journal Of Geophysical Research,111, doi:10.1029/2005JD006207.

Kishcha P., P. Alpert, A. Shtivelman, S.O. Krichak, J. H. Joseph, G. Kallos, P. Katsafados, C. Spyrou, G.P. Gobbi, F. Barnaba, S. Nickovic, C. Perez, and J. M. Baldasano, 2007: Forecast errors in dust vertical distributions over Rome (Italy): multiple particle size representation and cloud contributions. J. Geophys. Res. ï Atmospheres, 112, D15205, doi: 10.1029/2006JD007427

Klein H., S. Nickovic, W. Haunold, U. Bundke, B. Nillius, and co-authors, 2010: Saharan dust and ice nuclei over Central Europe. Atmos. Chem. Phys. 10, 10211-10221.

Klüser, L., D. Martynenko, and T. Holzer-Popp, 2011: Thermal infrared remote sensing of mineral dust over land and ocean: a spectral SVD based retrieval approach for IASI. Atmos. Meas. Tech. Discuss., 4, 461ï 509, doi:10.5194/amtd-4-461-2011

Knippertz, P. and M. C. Todd, 2010: The central west Saharan dust hot spot and its relation to African easterly waves and extratropical disturbances, J. Geophys. Res., 115, D12117, doi:10.1029/2009JD012819.

Knippertz, P., C. Deutscher, K. Kandler, T. Müller, O. Schulz, and L. Schütz, 2007: Dust mobilization due to density currents in the Atlas region: Observations from the Saharan Mineral Dust Experiment 2006 field campaign, J. Geophys. Res., 112, D21109, doi:10.1029/2007JD008774.

Leeuw, G., Neele, F. P., Hill, M., Smith, M. H., and Vignali, E., 2000 : Production of sea spray aerosol in the surf zone, J. Geophys. Res.Atmos., 105, 29397ï 29409.

Madronich, S., 1987 : Photodissociation in the atmosphere: 1. Actinic þux and the effects of ground reþections and clouds, J. Geophys. Res., 92, 9740ï 9752.

Marticorena, B. and Bergametti, G. 1995: Modeling the atmospheric dust cycle: 1. Design of a soil-derived dust emission scheme, J. Geophys. Res., 100, 16,415ï 16,430.

Mesinger, F., Chou, C.C., Gomes, L., Jovic, D., Bastos, P., Bustamante, J.F., Lazic, L., Lyra, A.A., Morelli, S., Ristic, I., Veljovic, and K., 2012: An upgraded version of the Eta model. Meteorol. Atmos. Phys., 116, pp. 63ï 79, doi 10.1007/s00703-012-0182-z, 2012

Miller, D.A and White, R. A., 1998 : A Conterminous United States Multilayer Soil Characteristics Dataset for Regional Climate and Hydrology Modeling, Earth Interactions ,2, Paper No. 2.

Miller, S. D., A. P. Kuciauskas, M. Liu, Q. Ji, J. S. Reid, D. W. Breed, A. L. Walker, and A. A. Mandoos, 2008: Haboob dust storms of the southern Arabian Peninsula, J. Geophys. Res., 113, D01202, doi:10.1029/2007JD008550.

Mlawer, E. J., Taubman, S. J., Brown, P. D., Iacono, M. J., and Clough, S. A., 1997: Radiative transfer for inhomogeneous atmospheres: RRTM, a validated correlated-k model for the longwave, J. Geophys. Res., 102 (D14) 16663ï 16682.

Monahan, E. C., Spiel, D. E., and Davidson, K. L., 1986 : A model of marine aerosol generation via whitecaps and wave disruption, in: Oceanic Whitecaps, edited by: Monahan, E. C. and Mac Niocaill, G., D. Reidel, 167ï 174.

Morcrette, J.-J., O. Boucher, L. Jones, D. Salmond, P. Bechtold, A. Beljaars, A. Benedetti, A. Bonet, J. W. Kaiser, M. Razinger, M. Schultz, S. Serrar, A. J. Simmons, M. Sofiev, M. Suttie, A. M. Tomplins, and A. Untch, 2009: Aerosol analysis and forecast in the ECMWF Integrated Forecast System: Forward modeling. J. Geophys. Res., 114, D06206, doi:10.1029/2008JD011235.

Nenes, A. and Seinfeld, J. H., 2003 : Parameterization of cloud droplet formation in global climate models, J. Geophys. Res., 108, 4415, doi:10.1029/2002JD002911

Nickovic, S., Kallos, G., Papadopoulos, A. and Kakaliagou, O. 2001 : A model for prediction of desert dust cycle in the atmosphere. J. Geoph. Res., 106, pp.18113-18129

Papadopoulos, A., Katsafados, P., Kallos, G., and Nickovic, S., 2002 : The Poseidon weather forecasting system ï An overview. The Global Atmosphere and Ocean Systems, 8, 219-237.
Papanastasiou D. K., A. Poupkou, E. Katragkou, V. Amiridis, D. Melas, and co-authors., 2010: An Assessment of the Efficiency of Dust Regional Modelling to Predict Saharan Dust Transport Episodes. Advances in Meteorology, 2010, 154368.
Pay M.T., M. Piot, O. Jorba, S. Gassó, M. Gonçalves, S. Basart, D. Dabdubd, P. Jiménez-Guerrero, and J. M. Baldasano, 2010: A Full Year Evaluation of the CALIOPE-EU Air Quality Modeling System over Europe for 2004. Atmospheric Environment, 44: 3322-3342
Pay, M.T., P. Jiménez-Guerrero, O. Jorba, S. Basart, X. Querol, M. Pandolfi, and J. M. Baldasano, 2012: Spatio-temporal variability of concentrations and speciation of particulate matter across Spain in the calliope modeling system. Atmospheric Environment, 46, 376-396
Perez C., Nickovic, S., Baldasano, J. M., Sicard, M., Rocadenbosch, F. and Cachorro, V. E., 2006 : A long Saharan dust event over the western Mediterranean: Lidar, Sun photometer observations, and regional dust modelling, J. Geophys. Res., 111, D15214, doi:10.1029/2005JD006579, 2006.
Pérez C., S. Nickovic, G. Pejanovic, J. M. Baldasano, and E. Ozsoy, 2006a: Interactive dust-radiation modeling: A step to improve weather forecasts. J. Geophys. Res., 111, D16206.
Pérez, C., S. Nickovic, J. M. Baldasano, M. Sicard, F. Rocadenbosch, and V. E. Cachorro, 2006b: A long Saharan dust event over the western Mediterranean: Lidar, Sun photometer observations, and regional dust modeling, J. Geophys. Res., 111, doi:10.1029/2005JD006579.
Pérez, C., K. Haustein, Z. Janjic, O. Jorba, N. Huneeus, J. M. Baldasano, T. Black, S. Basart, S. Nickovic, R. L. Miller, J. P. Perlwitz, M. Schulz, and M. Thomson, 2011: Atmospheric dust modeling from meso to global scales with the online NMMB/BSC-Dust model - Part 1: Model description, annual simulations and evaluation, Atmos. Chem. Phys., 12, 13001-13027, doi:10.5194/acp-11-13001-
Peyridieu, S., A. Chédin, D. Tanré, V. Capelle, C. Pierangelo, N. Lamquin, and R. Armante, 2010: Saharan dust infrared optical depth and altitude retrieved from AIRS: a focus over North Atlantic ï comparison to MODIS and CALIPSO, Atmos. Chem. Phys., 10, 1953-1967, doi:10.5194/acp-10-1953-2010
Schell B., Ackermann, I.J., Hass, H., Binkowski, F.S. and Ebel, A.: Modeling the formation of secondary organic aerosol within a comprehensive air quality model system, Journal of Geophysical research, 106, 28275-28293, 2001
Schulz, M., Balkanski, Y. J., Guelle, W. and Dulac, F.: Role of aerosol size distribution and source location in a three-dimensional simulation of a Saharan dust episode tested against satellite-derived optical thickness, J. Geophys. Res., 103, 10,579ï 10,592, 1998.
Shao, Y., Y. Yang, J. Wang, Z. Song, L.M. Leslie, C. Dong, Z. Zhang, Z. Lin, Y. Kanai, S. Yabuki, and Y. Chun, 2003: Northeast Asian dust storms: Real-time numerical prediction and validation, J. Geophys. Res., 108(D22), 4691, doi:10.1029/2003JD003667.
Solomos, S., Kallos, G., Kushta, J., Astitha, M., Tremback, C., Nenes, A., and Levin, Z.: An integrated modeling study on the effects of mineral dust and sea salt particles on clouds and precipitation. Atmos. Chem. Phys., 11, 873ï 892, doi:10.5194/acp11-873-2011, 2011.
Solomos, S., Kallos, G., Mavromatidis, E., and Kushta J.: Density currents as a desert dust mobilization mechanism, Atmos. Chem. Phys., 12, 11199-11211, 2012
Spyrou, C., Mitsakou, C., Kallos, G., Louka, P. and Vlastou, G.: An improved limited area model for describing the dust cycle in the atmosphere. Journal Of Geophysical Research, 115, D17211, doi:10.1029/2009JD013682, 2010.

Spyrou, C: Development Of Algorithms For The Calculation Of The Feedback Of Naturally Produced Particles Of Radiative Transfer And Energy Balance, 2011, University of Athens, PhD dissertation. Available at: http://phdtheses.ekt.gr/eadd/handle/10442/26160?locale=el

Spyrou, C., G. Kallos, C. Mitsakou, P. Athanasiadis, C. Kalogeri, and M. J. Iacono, 2013: Modeling the radiative effects of desert dust on weather and regional climate. ACP . www.atmos-chem-phys.net/13/5489/2013 doi:10.5194/acp-13-5489-2013

Todd, M. C., 2008: Quantifying uncertainty in estimates of mineral dust flux: An intercomparison of model performance over the Bodélé Depression, northern Chad. J. Geophys. Res., 113. ###-###

Uno, I., Z. Wang, M. Chiba, Y. S. Chun, S. L. Gong, Y. Hara, E. Jung, S.-S. Lee, M. Liu, M. Mikami, S. Music, S. Nickovic, S. Satake, Y. Shao, Z. Song, N. Sugimoto, T. Tanaka, and D. L. Westphal8, 2006: Dust model intercomparison (DMIP) study over Asia: Overview, J. Geophys. Res., 111, D12213,doi:10.1029/2005JD006575

Walcek, C. J., and Taylor, G.R.: A theoretical method for computing vertical distributions of acidity and sulfate production within cumulus clouds, J. Atmos. Sci., 43, 439ï 455, 1986.

Wesely, M. L., Parameterization of surface resistance to gaseous dry deposition in regional-scale numerical models, Atmos. Environ., 23, 1293-1304, 1989.

Zhang, K. M., Knipping, E. M., Wexler, A. S., Bhave, P. V., and Tonnesen, G. S.: Size distribution of sea-salt emissions as a function of relative humidity, Atmos. Environ., 39, 3373ï 3379, 2005.